



Published in final edited form as:

ACS Appl Mater Interfaces. 2021 May 12; 13(18): 20921–20937. doi:10.1021/acsami.1c01389.

## Anti-periprosthetic infection strategies: from implant surface topographical engineering to smart drug-releasing coatings

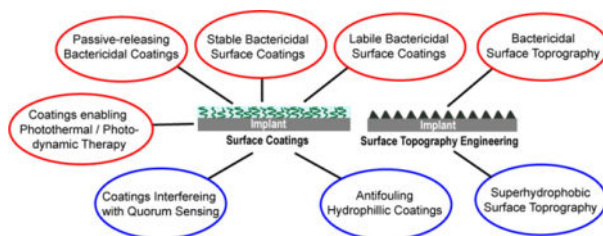
Ananta Ghimire<sup>a</sup>, Jie Song<sup>a,\*</sup>

<sup>a</sup>Department of Orthopedics and Physical Rehabilitation, University of Massachusetts Medical School, Worcester, Massachusetts, USA

### Abstract

Despite advanced implant sterilization and aseptic surgical techniques, periprosthetic bacterial infection remains a major challenge for orthopedic and dental implants. Bacterial colonization/biofilm formation around implants and their invasion into the dense skeletal tissue matrices are difficult to treat and could lead to implant failure and osteomyelitis. These complications require major revision surgeries and extended antibiotic therapies that are associated with high treatment cost, morbidity and even mortality. Effective preventative measures mitigating risks for implant related infections are thus in dire need. This review focuses on recent developments of anti-periprosthetic infection strategies aimed at either reducing bacterial adhesion, colonization and biofilm formation or killing bacteria directly in contact with and/or in the vicinity of implants. These goals are accomplished through anti-fouling, quorum sensing-interfering or bactericidal implant surface topographical engineering or surface coatings through chemical modifications. Surface topographical engineering of lotus-leaf mimicking superhydrophobic anti-fouling features and cicada wing-mimicking, bacterium-piercing nanopillars are both presented. Conventional physical coating/passive release of bactericidal agents is contrasted with their covalent tethering to implant surfaces through either stable linkages or linkages labile to bacterial enzyme cleavage or environmental perturbations. Pros and cons of these emerging anti-periprosthetic infection approaches are discussed in terms of their safety, efficacy and translational potentials.

### Graphical Abstract



### Keywords

Implant surface modifications; implant-related infections; surface topography; anti-fouling coatings; bactericidal coatings

\* jie.song@umassmed.edu.

## 1. Introduction

Any orthopedic surgical interventions involving implantation of biomaterials and application of fixation devices run the risk of implant related infections. Despite advancement in sterilization techniques and implementation of rigorous operating room protocols, the probability of periprosthetic joint infections (PJI), for instance, remains over 1% for primary arthroplasty and up to 30% in revision arthroplasty.<sup>1-4</sup> The elderly and immunocompromised patients are at a higher risk for acquiring implant related infections.<sup>5</sup> Once infected, treatment for PJI could require multi-stage revision surgeries involving the removal of the infected implant and extensive surgical debridement of the surrounding tissues prior to the insertion of a replacement implant. These revisions, even in combination with prolonged high-dose systemic antibiotic therapies, could still fail to rectify the problem and result in amputations or even deaths.<sup>6-11</sup> To date, no treatment strategies can guarantee the complete clearance of bacteria following PJI or prevent its recurrence.

Orthopedic implant related infections can be divided into three distinct categories based on the timing of infections with respect to implantation: early, delayed and late.<sup>12</sup> Risk of bacterial infection is typically highest immediately following implant placement, with early infections generally detected within 3 months of implantation and often associated with bacteria such as *S. aureus*.<sup>9</sup> This is due to the high tendency of implanted biomaterials, whether metallic alloys, polymers, ceramics or their combinations, to promote bacterial adhesion, colonization and the formation of biofilm, the dense extracellular matrices secreted by the colonized bacteria that are rich in viscous polysaccharides and proteins. The biofilm protects bacteria from host immune cells and is difficult to penetrate by conventionally administered antibiotics; it also prevents proper integration of the implant with surrounding tissues.<sup>13, 14</sup> Delayed infections are manifested between 3 and up to 24 months post implantation<sup>12, 15</sup> while late infection could occur >2 years post implantation. Delayed and late infections could result from either low-virulence bacteria like coagulase-negative *Staphylococci*<sup>9, 12</sup> or due to bacteria invasion of the canalicular network of surrounding bone, a safe haven protecting them from immune cells until their eventual release upon the destruction of the invaded bone matrices. This later scenario has been recognized as a major cause for the difficulty in effectively treating osteomyelitis caused by *S. aureus*.<sup>16</sup> Thus, development of implants with anti-fouling and/or bactericidal properties that minimize bacterial colonization and biofilm formation, timely eradicate them on implant surface and prevent their invasion and harboring within the periprosthetic tissue environment remains a top priority in combating periprosthetic infections.

Since the early 1970s, antibiotics have been incorporated into bone cement as local antibiotic prophylaxis in cemented total joint arthroplasty.<sup>17</sup> However, the high doses of antibiotics incorporated, coupled with their suboptimal release kinetics, present both safety and efficacy issues, with rapid burst releases risking local tissue toxicity while inadequate releases risking the development of antibiotic resistance.<sup>18, 19</sup> In addition, this strategy is not applicable to cementless orthopedics implants.<sup>20</sup> Considerable progress has been made in developing anti-periprosthetic infection surface modification strategies in the past 20 years.<sup>21-25</sup> Conceptually, these surface modifications can be divided into two main categories: anti-fouling/anti-quorum sensing (QS) modifications designed to discourage bacterial

adhesion/colonization/biofilm formation on surfaces in the first place (Figure 1A), and bactericidal modifications designed to kill bacteria in direct contact with the surface or in its vicinity (Figure 1B). They can be achieved by either implant surface topography engineering or chemical manipulations of implant surface coatings.<sup>26, 27</sup> In this review, we highlight key anti-fouling, QS-interfering and bactericidal implant surface modification strategies, used alone or in synergy, with an emphasis on those demonstrating *in vivo* promises for preventing or mitigating the severity of periprosthetic infections. An electronic search of Google Scholar and PubMed for literature describing implant surface modifications, implant related infection, anti-fouling surfaces, bactericidal surfaces, and smart drug delivery, published in English between 2000 and 2020, was performed. The results were then screened by title and abstract to only include those evaluating *in vivo* or *in vitro* efficacy of the surface modifications. Implant surface coatings of bactericidal metal ions, antibiotics and antimicrobial peptides (AMPs) via both stable covalent linkages and labile linkers cleavable by environmental triggers are presented. Pros and cons of these strategies, relative to conventional local and systemic antimicrobial deliveries, are discussed from both safety and efficacy perspectives. Strategies for regulating bacterial adhesion or viability through the alteration of mechanical properties (e.g. stiffness<sup>28</sup>) or chemical compositions (e.g. Zn and copper alloys<sup>29</sup>) of the bulk implant are not the subject of this review. Readers are also encouraged to refer to other recent reviews emphasizing the pathogenic mechanisms underlying implant-related infections<sup>30</sup>, biofilm dispersal strategies,<sup>31</sup> antimicrobial biomolecules,<sup>32</sup> or surface modification strategies specific to metallic implants<sup>33, 34</sup> including those focusing on mechanical/physical modification of the implants.<sup>35</sup>

## 2. Anti-fouling Implant Surface Modifications

Since adhesion is the first step of biofilm formation, thus understanding bacteria-surface interactions is essential for designing anti-fouling surfaces. Bacterial cells approach implant surfaces by different means, including Brownian motion, sedimentation, movement with liquid flow, bacterial motility with cell surface appendages, and interaction with other cells to form aggregates.<sup>36</sup> Bacterial attachment to the surface occurs through several mechanisms, among which hydrophobic and electrostatic interactions being the most common.<sup>37</sup> The type of predominant interaction varies from one bacteria to another and may even change upon mutations. Although no single theoretical model alone can accurately predict bacterial adhesion on different surfaces due to the complex nature of bacteria-surface interactions, altering surface topographical and physiochemical properties have been pursued extensively in designing anti-fouling surfaces.<sup>38–42</sup> Surface topography, roughness, hydrophilicity/hydrophobicity, and surface energy have all been recognized to play crucial roles in the initial adhesion of bacteria, non-specific adsorption of proteins and subsequent bacterial colonization and biofilm formation.<sup>43, 44</sup> Some of the anti-fouling strategies reviewed here draw their inspirations from nature, such as the self-cleaning texture in lotus leaf, the superhydrophobic butterfly wings, mosquito eyes and shark skins.<sup>45</sup> The anti-fouling surface topographical modifications discussed here involve changes in surface structures at atomic, molecular or textural levels.<sup>26, 46–48</sup> The anti-fouling surface coatings refer to the spreading and formation of an additional layer on the implant surface achieved physically, chemically or by a combination of both.<sup>49–51</sup> QS interference will also be

discussed as they constitute an alternative means of mitigating biofilm formation on implant surfaces.

## 2.1 Superhydrophobic Anti-fouling Surface Topography

Surface topography and chemistry are known to alter microbial attachment to substrates.<sup>39</sup> Generally, surface roughness promotes bacterial adhesion and subsequent biofilm formation due to increased total surface areas.<sup>52</sup> Theoretically, a bacterium will have a maximum number of attachment points when it fits perfectly within a micro-structured depression on a rough surface, which in turn may attract more cells to colonize around it, facilitating biofilm formation.<sup>53,54</sup>

However, surface topography changes may also be accompanied with changes in surface hydrophobicity, a phenomenon first observed with natural biological surfaces. For example, lotus leaves always appear clean despite their mire environment. The self-cleaning behavior of the lotus leaf was later attributed to its hierarchical micro-nanostructures and hydrophobic wax crystalloids on its surface.<sup>55, 56</sup> With air trapped within the rough surface topography, lotus leaf is superhydrophobic, significantly reducing the contact between water and the leaf surface as well as dirt particles and the leaf surface. When such a superhydrophobic surface tilts with a small sliding angle, water droplets roll off the surface with minimal spherical distortion, picking up loosely adhered foreign dirt particles as they roll.<sup>56</sup> Typically, when the sliding angle (beyond which water droplets freely roll) of superhydrophobic surface is lower than 10°, the surface is considered to possess self-cleaning property.<sup>57</sup> By contrast, a more spread water droplet on the normal surface just passes over the dust upon surface tilting.

Mimicking the lotus leaf self-clearing effect, superhydrophobic surfaces have been designed to reduce bacterial adhesion.<sup>58</sup> Surface hydrophilicity or hydrophobicity is generally measured as liquid contact angle ( $\theta$ ) (equation 1)

$$\cos(\theta) = \frac{\gamma_{sv} - \gamma_{sl}}{\gamma_{lv}} \quad (1)$$

where  $\theta$  is Young's contact angle,  $\gamma$  is the surface tension and s, l, and v represent solid, liquid and vapor, respectively. A water contact angle of 0° means complete wetting while a contact angle of 180° means that water does not wet the substrate surface. In general, a surface with a water contact angle of >150° is considered superhydrophobic.<sup>5, 45</sup> These surfaces exhibit significantly low adhesion forces to hydrophilic liquids like water, causing droplets to roll over with minimal distortions when tilted. During this process, bacteria and other particles on surface will presumably be removed along with the rolling liquid droplet much like dusts on the lotus leaf. To test this hypothesis, superhydrophobic surfaces were designed and tested for their anti-fouling capacity.<sup>56</sup>

Tang *et al.*<sup>59</sup> studied the adhesion of *S. aureus* on medical grade titanium surface-engineered with varying wettability through the generation of nanotube structured TiO<sub>2</sub> surface films using electrochemical oxidation and self-assembly techniques. Specifically, the titanium were treated by surface anodic oxidation only (NT), perfluorooctyltriethoxysilane (PTES)

only (TiS), or PTES following the anodic oxidation (NTS), resulting in hydrophilic (water contact angle of 54°), hydrophobic (water contact angle of 133°), and superhydrophobic (water contact angle of 156°) surfaces, respectively. Figure 2 shows that although *S. aureus* adhered on all three surfaces after 2–4 h *in vitro* incubation, they were far more scattered on the hydrophobic and superhydrophobic surfaces, especially on the latter.

Besides the superhydrophobic micro- and nano-scaled surface topographical features, bacterial surface adhesions are also found to be affected by bacterial shape. For example, Fadeeva *et al.*<sup>58</sup> used femtosecond laser ablation technique to produce superhydrophobic self-organized micro- and nano-structures mimicking those of the lotus leaf on titanium surfaces. The water contact angle was increased up to 166° upon the surface laser treatment (vs. 73° of the polished surface). Whereas the biomimetic superhydrophobic surface resisted the adhesion of rod-like *P. aeruginosa*, spherical *S. aureus* cells were found to still colonize on the superhydrophobic surface. The authors suggested that the spherical *S. aureus* may have required less attachment points to adhere on the surface compared to *P.aeruginosa*. Biophysical mechanisms underlying this phenomenon will need to be further investigated.

It should be noted that the air trapped within the periodical, lotus leaf-like micro/nano-structured topographical features plays a significant role in affording these surfaces anti-fouling properties. Huang *et al.*<sup>60</sup> showed increased non-specific protein adsorption on superhydrophobic surface TiO<sub>2</sub> nanotubes in the absence of the trapped air. Thus, the duration/longevity of the anti-fouling capabilities of such topographically engineered superhydrophobic surfaces in an aqueous physiological environment is a legitimate concern for their *in vivo* applications as the trapped air will eventually get excluded from the engineered surface over time.

## 2.2 Hydrophilic Anti-fouling Surface Coatings

Applying hydrophilic antifouling coatings to implants may also reduce bacterial attachment and biofilm formation by enabling the formation of a surface hydration shield<sup>37, 61–65</sup> (Figure 1A, top left). This is in contrast to the superhydrophobic surfaces that prevent biofouling by facilitating the ready detachment/cleaning of loosely adsorbed proteins or bacteria. Although the hydrophilic surface coatings are not bactericidal in nature, they are particularly effective in minimizing the initial bacteria-implant interactions. Non-ionic poly(ethylene glycol) (PEG), amphiphilic fluoropolymers, and zwitterionic polymers are among the most common hydrophilic polymers explored as anti-fouling surface coatings.<sup>56, 66–68</sup> Negatively charged polymers such as heparin, on the other hand, was shown to be able to promote biofilm formation by substituting extracellular DNA secreted by *S. aureus*,<sup>69</sup> thus should be used with caution.

**2.2.1 PEG Coating**—PEG has long been appreciated for its anti-fouling properties and has been reviewed extensively.<sup>40, 70, 71</sup> Each ethylene glycol repeating unit in PEG can strongly bind to one water molecule via H-bonding, with structural water molecules bridging the ether oxygens along the helical PEG chain.<sup>72–74</sup> This results in a highly hydrated layer that serves as a steric barrier to approaching biofoulants such as proteins or bacteria.<sup>75</sup> The high mobility and large exclusion volume of PEG chains further contribute towards the anti-

fouling nature of PEG-coated surfaces.<sup>40</sup> Khoo *et al.*<sup>76</sup> used a high affinity titanium-binding 22-mer peptide containing three repeats of HKH to graft PEG on a titanium surface. This peptide selectively binds titanium with sub-micromolar binding affinities over stainless steel, gold, polystyrene, or SiO<sub>2</sub>. The PEGylated-peptide coating on titanium surface efficiently blocked the adsorption of fibronectin and significantly reduced the extent of *S. aureus* attachment *in vitro*. Buxadera-Palomero *et al.*<sup>77</sup> compared the anti-fouling properties of PEG-coated titanium surface prepared using three different techniques, plasma polymerization, electrodeposition and silanization. All three coatings significantly reduced non-specific protein adsorption (bovine serum albumin) and bacterial (*S. sanguinis* and *Lactobacillus salivarius*) adhesion. The tendency of PEG to be oxidized under sterilization conditions or *in vivo*<sup>78, 79</sup> in the presence of oxygen and transition metal ions,<sup>80, 81</sup> however, could lead to its eventual fouling and compromise their long-term anti-fouling performances.

**2.2.2 Zwitterionic Coating**—Zwitterionic polymers have been explored as alternative anti-fouling surface coatings due to their improved oxidative stability over PEG. Zwitterionic materials are characterized with an equal number of positively and negatively charged residues that maintain an overall electrical neutrality. The strong dipoles and electrostatic interactions of these charged residues facilitate the formation of a tightly bound hydration layer resisting biofoulant deposition. Naturally occurring zwitterionic lipid phosphatidylcholine that constitutes a significant fraction of the outer membrane of many cell types has long been recognized for its anti-fouling properties (e.g. anti-thrombogenic properties of the outer membrane of erythrocyte<sup>82, 83</sup>). Inspired by the zwitterionic membrane lipid, researchers have explored phosphorylcholine-based polymers<sup>84</sup> and synthetic zwitterionic polymers to create anti-fouling surfaces for resisting bacterial adhesion.<sup>85–89</sup> For example, Cheng *et al.*<sup>89</sup> showed that zwitterionic poly(sulfobetadine methacrylate) (pSBMA) coated on gold or glass surfaces inhibited both Gram-positive (*S. epidermis*) and Gram-negative (*P. aeruginosa*) bacteria adhesion and biofilm formation *in vitro*. For orthopedic applications, another potential advantage of applying zwitterionic coatings as opposed to their non-ionic counterparts (e.g. PEG) to implant surfaces is the unique ability of zwitterions to attract oppositely charged precursor ions under pro-mineralization conditions, thereby promoting templated biomineralization and osteointegration as we demonstrated on both 2D surfaces<sup>90</sup> and within 3D matrices.<sup>91, 92</sup>

### 2.3 Synergy of Anti-fouling Coating and Systemic Delivery of Antibiotics

One limitation of anti-fouling coatings is that they are not bactericidal, thus cannot eradicate infections in the periprosthetic tissue environment. We recently demonstrated that zwitterionic anti-fouling implant coatings, however, can significantly enhance the efficacy of systemic antibiotic injections in combating periprosthetic infections.<sup>93</sup> We first confirmed that zwitterionic polymer brush pSBMA surface-grafted from Ti6Al4V (Ti-pSBMA) significantly reduced *S. aureus* adhesion both *in vitro* and *in vivo*. However, Ti-pSBMA intramedullary (IM) pin inserted in *S. aureus*-inoculated murine femoral canal expectedly did not kill the bacteria to prevent bone infections, as evidenced by the significant increase in cortical thickness (Ch. T.) and reductions in bone volume fraction (BVF) and bone mineral density (BMD) compared with uninfected control femurs (Figure 3). Meanwhile, a single systemic vancomycin injection 7 days after inserting an uncoated IM pin into the *S.*

*aureus*-inoculated femoral canal (Ti6Al4V+VAN) also failed to prevent bone infections. However, when the pSBMA coating was combined with the single systemic vancomycin injection (Ti-pSBMA+VAN), it significantly inhibited both *S. aureus* colonization on implant surface and periprosthetic infections in the mouse femur (vs. Ti-pSBMA or Ti6Al4V+VAN, Figure 3). This study showed that the anti-fouling coating, by suppressing bacterial colonization/biofilm formation on implant surfaces, could make the planktonic bacteria within the periprosthetic tissue environment more susceptible to conventional systemic antibiotic treatment, thereby improving the efficacy and safety (reduced dose and frequency) of such treatments.

## 2.4 Coatings Interfering with Quorum Sensing (QS)

QS is a population density dependent cell-cell signaling that triggers changes in behavior when the population reaches a critical density.<sup>94, 95</sup> In QS, bacteria produce and release chemicals termed autoinducers as a common signal whose external concentration increases with bacteria population density. Bacterial cells detect these changes and when minimal threshold stimulatory concentration of these autoinducers are reached, they alter gene expressions and behavior in response.<sup>95</sup> In recent years, various QS inhibitors such as cinnamaldehyde,<sup>96, 97</sup> hamamelitannin,<sup>98</sup> baicalin,<sup>99</sup> silver nitrate, furanone C-30<sup>100, 101</sup> have been used to interfere and disrupt the signaling processes in bacterial growth and subsequent biofilm formation. Kang *et al.*<sup>101</sup> used poly(butyl methacrylate-co-methacryloyloxyethyl phosphate) (PBMP)/PLGA microparticles encapsulating furanone C-30 on hydroxyapatite (HA) surfaces to prevent biofilm formation. PBMA contains Ca<sup>2+</sup>-binding phosphomonoester groups to ensure good adherence to the HA surface and the PLGA-interacting butyl groups to encapsulate furanone C-30. The C-30-bearing PLGA/PBMP microparticles effectively inhibited the growth of *Streptococcus mutans* and its ability to form biofilms on HA surface for up to 100 h, which was much longer than either furanone C-30 in its free form or when encapsulated in PLGA microparticles.

However, the use of QS interference as a potential therapeutic approach against biofilm formation has its own challenges. Despite the shared QS mechanism among various bacteria, it is often a species-specific process.<sup>102</sup> The primary translational challenge will be to design and synthesize agents that interfere and disrupt QS across a diverse range of bacterial species.

## 3. Bactericidal Implant Surface Modifications

The interest in biomaterials exerting bactericidal activities has seen an upsurge in recent decades. The bactericidal activities can be endowed via surface topography engineering and/or bactericidal agents covalently tethered to stable coatings or released from labile coatings.

### 3.1 Bactericidal Surface Topography

Micro/nano scale surface topography can not only be engineered to inhibit bacterial adhesion and growth but also to physically lyse bacterial cells. The initial concept of nanostructured bactericidal topography originated from the unique nano pillar patterns of

Cicada (*Psaltoda claripennis*) wings that were postulated by Ivanova *et al.*<sup>103</sup> to mechanically rupture bacterial cell walls. Later, Kelleher *et al.*<sup>104</sup> studied three subspecies of cicada wings, *Megapomponia intermedia*, *Ayuthia spectable*, and *Cryptotympana agulia*, and found strong correlations between their bactericidal properties and their nanoscale surface topographies. Sharper and denser nanopillars on the *Megapomponia intermedia* wings were found to kill bacteria more efficiently, probably by inducing greater strains on the bacterial cell wall. Since this discovery, biomimetic bactericidal nanostructured surface architectures have been engineered with various biomaterials including titanium and its alloys.<sup>105–112</sup>

For example, Diu *et al.*<sup>107</sup> investigated bactericidal properties of nanowires grown on titanium surfaces using an alkaline hydrothermal method. It was found that motile and Gram-negative bacteria are more susceptible to the killing by these surfaces compared to nonmotile and Gram-positive ones. The lack of mobility and the thicker cell wall found in Gram-positive bacteria have likely made them more resistant to being mechanically ruptured. Similar observations were reported by Sengstock *et al.*<sup>111</sup> on titanium nanocolumnar surface structures produced using a glancing angle sputter deposition technique. It was observed that the Gram-negative, rod-shaped *E. coli* were killed more readily compared to the Gram-positive, sphere-shaped *S. aureus*. Apart from the cell wall difference, *E. coli* multiplies by elongation which requires in-plane movement of the bacterium attached to the surface nanostructures. The frictional force during cell division could result in damage or disruption of the cell wall. *S. aureus*, on the other hand, divides in three dimensions, leading to grape-like clusters or out of plane growth. This resulted in fewer daughter *S. aureus* cells in direct contact with the nanocolumnar titanium surface during the cell division, thus fewer cell death. Hasan *et al.*<sup>105</sup> used a chlorine based reactive ion etching process to generate titanium nanopillars or black titanium. Within 4 hours of contact with the black titanium surface, 95±5% of *E. coli*, 98±2% of *P. aeruginosa*, 92±5% of *M. smegmatis* and only 22±8% of *S. aureus* attached were killed. The killing efficiency of the black titanium for *S. aureus* increased to 76±4% when the bacteria were allowed to adhere for 24 h (Figure 4).

The exact mechanisms of the bactericidal effect of these nanostructures are still under investigation. Besides the widely used explanation of physical deformation or rupturing of bacterial cell wall by the sharp nanostructures,<sup>113</sup> physical entrapment of bacteria in-between the nanostructures may have also contributed to impeding their proliferation.<sup>109</sup> The frictional forces exerted on the cell wall of Gram-negative bacteria during the cell division is another contributing factor to the bacterial cell death.<sup>111</sup> A unique challenge for such bactericidal surface topographies to be implemented *in vivo* is to ensure their abilities to still support osteointegration. A typical reduction in bone cells proliferation on surfaces engineered with bactericidal topographies with high aspect ratio compared to unmodified implant surfaces has been reported.<sup>105, 107</sup> A potential solution is to further functionalize these higher aspect ratio bactericidal topographies with cell receptor binding molecules. For example, Fraioli *et al.*<sup>114</sup> used integrin-binding peptides to functionalize the bactericidal topographies to improve the adhesion of mesenchymal stem cells (MSCs) while preserving its bactericidal properties against *P. aeruginosa*. The *in vivo* efficacy of this approach as well as the universal adaptability (against different types of bacteria as well as “protection” against various host cells) remain established.



### 3.2 Stable Bactericidal Surface Coatings

Small molecule bactericidal agents and AMPs have been covalently attached to implant surfaces to enable contact killing of bacteria.<sup>71, 115</sup> In this approach, bactericidal agents are often tethered to the surface via either a flexible linker or a polymer for contact killing, with the latter ensuring its penetration through the thick bacterial cell wall to reach and disrupt the cytoplasmic membrane (e.g. by polycations).<sup>116</sup>

Vancomycin, for instance, has been covalently tethered to surfaces for contact killing by inhibiting cell wall synthesis via direct binding to the peptidoglycan stem unit within the cell wall. For instance, Edupuganti *et al.*<sup>117</sup> demonstrated that a monolayer of vancomycin covalently attached to Ti6Al4V pin surfaces via a bis(ethylene glycol) linker was effective in reducing *S. aureus* colonization *in vitro*. Similarly, Antoci *et al.*<sup>118</sup> showed that a monolayer of vancomycin covalently attached to Ti6Al4V IM pin surfaces via an ethylene glycol linker was effective in reducing the bacterial colonization of *S. aureus in vitro* and *in vivo* and mitigated the severity of osteolysis of the surrounding bone in the short term. The rodent femur receiving the bacterial inoculation and unmodified titanium pin implant showed extensive periosteal reactions, enlargement of the IM canal, compromised cortical bone integrity, and extensive abscess formation after 14 days that are characteristic of periprosthetic infections/osteomyelitis. In contrast, the femur inoculated with the bacteria but inserted with the vancomycin modified IM pin showed minimal disruption of the surrounding bone by 14 days. However, the monolayer of tethered antibiotics is limited by the achievable drug density and was only able to provide limited short-term protection.<sup>118</sup>

To overcome the limited surface density of bactericidal agents achievable by monolayer functionalization, we grafted polymers with vancomycin-terminated sidechains from Ti4Al4V implant<sup>22</sup> to significantly reduce the colonization/growth of *S. aureus* on the implant surface. Alkynylated vancomycin was covalently coupled through copper-catalyzed azide-alkyne cycloaddition to the azide-terminated sidechains of polymethacrylates grafted from Ti6Al4V by surface-initiated atom transfer radical polymerization. Using a mouse femoral canal *S. aureus* infection model, we showed that with the vancomycin-bearing polymer coating, the IM pins inserted in the femoral canal significantly suppressed *S. aureus* colonization on the implant surface (68 CFU/pin) compared to unmodified pins (~1500 CFU/pin), >20-fold reduction, by 3 weeks. Furthermore, we showed that the bacterial counts from the retrieved pins remained low after 4 months, with 3 out of the 4 pins evaluated showing 0 CFU while one showing low counts (50 CFU/pin). However, this surface treatment did not prevent the infection from being developed in the surrounding bony tissue, underscoring the short-range protection by the vancomycin covalently tethered to surface polymer coating.

Zeng *et al.*<sup>119</sup> designed an antibacterial and anti-fouling polymeric coating via a one-pot ring-opening reaction of antibiotic gentamycin and ethylene glycol species. The PEG moieties provided anti-fouling properties whereas the gentamycin exhibited antibacterial activities against both *S. aureus* and *E. coli*. However, this bifunctional surface coating still faced the same limitation of restricting the antibacterial activities to the immediate surface of the implant.

AMPs have been explored as a promising alternative to antibiotics in combating implant related infections because of its high potency against a broad spectrum of bacteria and lower propensity to develop antibacterial resistance.<sup>71, 120</sup> Chen *et al.*<sup>121</sup> silanized titanium surfaces with an alkyne-terminated linker, which was then conjugated with azido-functionalized cationic AMP (N<sub>3</sub>-PEG<sub>12</sub>-KRWWKWR) by copper catalyzed alkyne-azide cycloaddition (CuAAC). The AMP-modified surface exhibited 88–90% inhibition against *S. aureus* and *E. coli* within 2.5-h *in vitro* incubation, and the bactericidal activity declined over longer incubations. The modified surfaces exerted some degree of cytotoxicity against murine MSCs in an AMP-dose dependent manner over 24-h culture. Using a rabbit tibial metaphysis drill-hole (3-mm) model infected with *S. aureus* (5×10<sup>6</sup> CFU inoculation), the AMP-coated implant was shown to mitigate (although not eradicate) the periprosthetic infection after 7 days compared to that treated with the uncoated control implant. Longer-term bactericidal activity as well as potential cytotoxicity of the AMP coating against host cells need to be further evaluated. Godoy-Gallardo *et al.*<sup>122</sup> used atom transfer radical polymerization to covalently attach a human lactoferrin protein-derived peptide hLF1–11, where the cationic AMP was functionalized with three 6-aminohexanoic acid (Ahx) residues as the spacer and a 3-mercaptopropionic acid (MPA) as the anchoring group [MPA-Ahx-Ahx-Ahx-GRRRRSVQWCA-NH<sub>2</sub>], to titanium surfaces. These AMP-modified surfaces exhibited good inhibition of oral bacteria *S. sanguinis* and *L. salivarius* attachment and biofilm progression *in vitro*. However, the scope (human foreskin fibroblasts used) and duration of the cytocompatibility evaluation (24 h) of the coating was quite limited, and the *in vivo* bactericidal properties are yet to be evaluated. Given the potential interaction/disruption of cationic AMPs with/to the negatively charged primary cell membranes, rigorous long-term cytocompatibility evaluations with a broad range of host cells surrounding the implant and *in vivo* biocompatibility evaluations of such coatings would be essential for their safe translational applications.

### 3.3 Labile Bactericidal Surface Coatings

An alternative approach for reducing implant related infections is through implant coatings that can release bactericidal agents.<sup>123, 124</sup> The greatest benefits of such local release of bactericidal agents are the enhanced efficacy due to higher achievable local concentrations,<sup>125, 126</sup> minimized systemic side effects, and the ability of the released bactericidal agents to diffuse into the periprosthetic tissue environment, thereby killing bacteria on both the implant surface and within the surrounding tissue environment. The effectiveness of these coatings is strongly dependent on the release kinetics of the bactericidal agents.

**3.3.1 Metal ion Releasing Coatings**—Silver/silver nitrate has been used to treat burns and chronic wounds (e.g. ulcers) for centuries.<sup>127, 128</sup> Although silver-based treatment of bacterial infections declined after penicillin was introduced in the 1940s,<sup>129, 130</sup> Moyer *et al.*<sup>131</sup> reintroduced 0.5% silver nitrate solution to treat burn wounds in the 1960s as it was found to exert broad antibacterial property against *S. aureus*, *P. aeruginosa*, and *E. coli* without interfering epidermal cell proliferation. Indeed, silver/silver ion-bearing coatings have continued to attract attentions due to their broad-spectrum antimicrobial effects on both Gram-positive and Gram-negative bacteria. Although silver is chemically stable, silver ion is highly reactive and can incapacitate bacteria by binding to proteins (e.g. thiol-containing

enzymes), permeating bacterial cell wall, and causing DNA condensation.<sup>132</sup> Yavari *et al.* showed that silver nitrate loaded on porous titanium implant surfaces (TiO<sub>2</sub> nanotubes) effectively prevented *S. aureus* biofilm formation and decreased the number of planktonic bacteria *in vitro*, especially at adequate loading concentrations.<sup>133</sup> Li *et al.* also showed that porous titanium loaded with silver (Ag<sup>0</sup>)-bearing gelatin microspheres inhibited bacterial growth of both *S. aureus* and *E. coli*.<sup>134</sup>

Copper/copper (II) ions also exhibit broad spectrum antibacterial activities against microorganisms such as *S. aureus*, *E. coli*, *S. enterica*, *C. jejuni*, and *M. tuberculosis*.<sup>135–137</sup> In addition to the bactericidal effect, an appropriate dose of Cu<sup>2+</sup> could also promote angiogenesis and osteogenesis.<sup>137, 138</sup> Wang *et al.*<sup>139</sup> studied the bactericidal activity of Cu<sup>2+</sup>-deposited titanium prepared using a polydopamine (PDA)-assisted surface modification technique. The obtained Ti-PDA-Cu substrate exhibited excellent antibacterial activity against *S. aureus* and promoted osseointegration in a rat tibia infection model.

Zinc/zinc (II) ions have also been exploited to combat orthopedic/dental implant related infections. Li *et al.*<sup>25</sup> modified titanium surfaces with ZnO nanorods followed by polydopamine (PDA) and cell adhesive RGDC peptide. Using a *S. aureus*-infected rabbit femoral unicortical drill hole model, the Ti/ZnO/RGDC hybrid implant coating was shown to improve antibacterial efficacy, resulting in far less neutrophils and adherent bacteria in the surrounding tissue. The coating also accelerated new bone formation and implant osteointegration compared to unmodified titanium implant. Without additional controls, however, it is difficult to delineate the bactericidal contribution due to the physical puncturing of the bacteria by ZnO nanorods from that of the released Zn<sup>2+</sup> or the osteogenic role of Zn<sup>2+</sup> from that of PDA/RGDC.

Different mechanisms have been proposed to explain the bactericidal activity of metal ions. It has been suggested that the binding of metal ions to bacterial cell membrane, the primary site of action,<sup>140, 141</sup> creates pits and holes.<sup>142</sup> The increased bacterial membrane permeability results in leakage of intracellular material, shrinkage of cell membrane, and ultimately cellular lysis.<sup>143</sup> The metal ions could also interfere with the bacterial gene replication and promote the generation of bacteria-killing reactive oxygen species (ROS).<sup>144–146</sup> For example, Li *et al.*<sup>146</sup> investigated the mechanism of *S. aureus* inactivation by Cu<sup>2+</sup> ions released from Ti6Al4V5Cu alloy. In addition to the disruption in bacterial cell membrane permeability, they observed an increase in ROS production and the interference to the replication of nuc (species-specific) and 16SrRNA genes (Figure 5). Finally, microbial susceptibility to Zn<sup>2+</sup> toxicity is shown to be mediated by extracellular cation competitions that result in the inhibition of the bacterial acquisition of essential metal ions such as Mn<sup>2+</sup> by competing for binding to solute binding proteins.<sup>147</sup>

Despite the promises of these metal ion-based coatings for combating implant related infections, it remains controversial whether metal ion-mediated antibacterial activity may be inactivated in physiological fluids<sup>148</sup> and whether a sublethal concentration of ions like silver is a cause of concern for the development of drug resistance. Another important translational consideration for this strategy is the potential cytotoxicity of the metal ions exerted to host periprosthetic tissues/cells.<sup>149,150</sup>

**3.3.2 Antibiotics Releasing Coatings**—Local release of antibiotics,<sup>151</sup> if accomplished timely and in adequate yet not excessive concentrations, could directly target peri-implantitis bacteria without significant systemic side effects.<sup>152</sup> A broad range of synthetic polymers such as PLGA,<sup>153</sup>  $\alpha$ - $\omega$ -functionalized PEG nanoparticles and hydrogels,<sup>154, 155</sup> poly(2-hydroxyethyl methacrylate) (pHEMA),<sup>156</sup> and heparin-dopamine<sup>157</sup> have been used for localized antibiotics delivery. The effectiveness of an antibiotics-releasing system depends strongly on the rate and manner in which the drug is released, which in turn is dictated by the degradative properties of the polymeric coating or the responsiveness of the labile linkage tethering the antibiotics to its environmental trigger. Both hydrolytic degradation of polymer/hydrogel coatings and the cleavage of labile linkers sensitive to stimuli like pH or host/bacterial enzymes (e.g. nuclease and/or hyaluronidase) have been utilized.<sup>21, 158–160</sup> Here we review a few bactericidal implant coatings based on passive, physical stimuli triggered, or enzyme triggered release of antibiotics.

**3.3.2.1 Passive Release:** Passive drug release systems utilize diffusion, osmotic potential, or concentration gradients as the driving forces for drug release from the coating material. For example, antibiotics release from polymethylmethacrylate bone cements is mainly achieved by diffusions through surface roughness, superficial pores, and surface erosion.<sup>161, 162</sup> Stigter *et al.*<sup>163</sup> studied the release of carbenicillin, amoxicillin, cefamandole, tobramycin, gentamicin and vancomycin from carbonated hydroxyapatite coatings on titanium surfaces, with all showing inhibition of *S. aureus* growth. PLGA is also widely used as an antibiotic carrier because of its excellent biocompatibility and hydrolytic degradability *in vivo*.<sup>164</sup> Antibiotics embedded in PLGA coatings can be released by both diffusion and through the hydrolytic degradation of the polymer. For example, Yeh *et al.*<sup>153</sup> used plasma spraying to coat PLGA loaded with vancomycin and cefuroxime on Ti6Al4V surfaces. At an optimized loading dose, the PLGA coating released 8% of the cefuroxime in the first 24 h followed by a slower, continuous release over a period of 17 days. The initial burst release was due to diffusion while the subsequent slower release was due to diffusion under the influence of PLGA degradation. However, such passive bactericidal agent releasing systems may not be adequate for achieving rapid clearance of active infections. Furthermore, the slow, continued release of antibiotics from these coatings may also increase the risk for developing bacteria resistance,<sup>18, 19, 165–167</sup> which is a huge concern for both Gram-positive and Gram-negative bacteria.

**3.3.2.2 Physical Stimuli Triggered Release:** Stimuli-responsive materials have been investigated in the biomedical field for several decades including as drug release systems.<sup>168</sup> Polymers or polymeric hydrogels can undergo volume changes, structural transformations or covalent bond cleavages in response to certain stimuli, causing subsequent release of encapsulated/tethered antibiotics.<sup>168</sup> Physical stimuli such as pH, temperature, magnetic field, and ultrasound have all been used to trigger the release of bactericidal agents.<sup>169–175</sup>

As bacterial metabolism produces lactic acid and acetic acid, the pH drops in the vicinity of bacterial infections can be used to trigger the release of bactericidal agents. Chemical bonds such as Schiff base,<sup>176</sup> acetal linkage<sup>177</sup> and metal ion coordination bonds<sup>159, 174, 178</sup> that are stable under neutral conditions but labile at lower pH are often utilized to realize the pH-

triggered release. Wang *et al.*<sup>159</sup> designed a pH-responsive coordinated polymer (CP) / amine-functionalized titania nanotubes (TNTs-NH<sub>2</sub>) coating for titanium implants. The nanotubes were first filled with drugs like ibuprofen, vancomycin or Ag and then capped by CPs formed by 1,4-bis(imidazole-1-ylmethyl) benzene and Zn<sup>2+</sup> or Ag<sup>+</sup>, where the metallic ions acted as coordination bonds between the polymer and the amino groups of the TNTs-NH<sub>2</sub>. Under acidic conditions, the coating released Zn<sup>2+</sup> or Ag<sup>+</sup> as a result of the protonation of the amino groups and the weakening of the coordination bonds, exerting local antibacterial activities. Tao *et al.*<sup>179</sup> deposited levofloxacin (Levo)-loaded zeolitic imidazolate framework-8 (ZIF-8@Levo) nanoparticles onto collagen-modified titanium substrates by cathode electrophoresis deposition. ZIF-8, a metal organic framework based on Zn<sup>2+</sup>-imidazole coordination, can fall apart under acidic pH to release its drug contents as well as the bactericidal Zn<sup>2+</sup>. Gelatin and chitosan multilayers were spin-coated layer by layer (ZIF-8@Levo/LBL) to reduce the hydrolysis rate of ZIF-8@Levo. ZIF-8, ZIF-8@Levo and ZIF-8@Levo/LBL coatings all exhibited bactericidal properties against *E. coli* and *S. aureus in vitro*. Using a rat femoral canal *S. aureus* infection model, metal pins with these coatings were also shown to significantly reduce bacterial counts on both the implant and in surrounding bone compared to uncoated implants or those only coated with type I collagen. The benefit of the LBL coating on the drug release control, however, was not adequately reflected in this study.

Unlike the background leaching often observed with pH-triggered releases,<sup>180</sup> ultrasound triggered release could lead to more rapid release far above the background when the coating is designed to minimize passive release. Noble *et al.*<sup>181</sup> achieved low background leaching of ciprofloxacin from pHEMA by co-polymerizing it with hydrophobic monomer hydroxypropyl methacrylate and further coating it with self-assembled multilayers of C12–C18 methylene chains that were predominantly crystalline and relatively impermeable. These added layers acted as a barrier for both water diffusion to and antibiotic release from the hydrogel. Upon ultrasound triggering, the ciprofloxacin release 14-fold more intense than background level was achieved.

**3.3.2.3 Bacterial Enzyme Triggered Release:** On demand release of antibiotics has the potential to provide timely protection of the periprosthetic tissue environment from infection while minimizing the risk for developing bacterial resistance by avoiding unwanted release of antibiotics. Proteases, lipases and nucleases have all been explored for the triggered release of antibiotics and antimicrobial agents. Johnson *et al.*<sup>182</sup> engineered a PEG hydrogel for protease-triggered delivery of lysostaphin, an antimicrobial enzyme targeting the peptidoglycan of staphylococci and a known inhibitor of the growth of methicillin-resistant *S. aureus* (MRSA), to treat *S. aureus* infected, implant-fixed mouse femoral fractures. The hydrogels were prepared by mixing four-arm PEG macromers functionalized with terminal maleimide groups (PEG-4MAL), protease-degradable 16-mer peptide crosslinker with terminal cysteines, and thiolated cell adhesive peptide RGD or GFOGER, with or without lysostaphin. The lysostaphin encapsulated in the hydrogel was shown to outperform prophylactic antibiotic or soluble lysostaphin therapy in reducing the infection in this model. However, the protease-triggered release of lysostaphin was not dependent on the presence of

bacteria; its cleavage by host proteases would not have prevented undesired releases of the antimicrobial agent.

Wang *et al.*<sup>160</sup> designed vertically aligned mesoporous silica coating on the surface of stainless steel for pH- and bacterial lipase-triggered antibiotic release. Alkyne-terminated surface linkers were conjugated to the mesoporous silica coating via sequential amidation and esterification. After loading antibiotics cinnamaldehyde and ampicillin into the perpendicular mesochannels,  $\beta$ -cyclodextrins functionalized with monopyridine and azides were covalently tethered to the alkyne-terminated surface linkers using azide-alkyne cycloaddition “click” chemistry, resulting in the “capping” of antibiotic-loaded mesochannels by the monopyridine-functionalized cyclodextrin. It was demonstrated that the lowering of pH triggered the opening of the cyclodextrin “valve” by reorienting the monopyridine from the interior of the cyclodextrin to the exterior, enabling the release of the smaller antibiotic cargo cinnamaldehyde. Meanwhile, lipase was shown to cause the irreversible cleavage of the functionalized cyclodextrin, leading to the release of both antibiotic cargos. This dual release system was shown to inhibit the growth of *S. aureus*, *E. coli* and MRSA *in vitro*. It is unclear, however, whether the lipase-triggered cleavage may be confounded by the presence of host lipase activities *in vivo* due to the lack of specificity in the labile linker design.

Yuan *et al.*<sup>158</sup> applied catechol-functionalized multilayer coatings composed of dopamine-modified hyaluronic acid and 3,4-dihydroxyhydrocinnamic acid-modified chitosan to titanium surfaces modified with TiO<sub>2</sub> nanotubes (TNT) filled with vancomycin. The coating was designed to release vancomycin upon cleavage of hyaluronic acid by elevated hyaluronidase activities in the presence of bacterial infections. Using a rat femoral canal *S. aureus* infection model, the titanium IM implant applied with such coating was shown to mitigate the infections. Subsequently, this group<sup>183</sup> also applied hyaluronic acid-gentamicin conjugates and chitosan polyelectrolyte multilayer coatings on deferoxamine (DFO) loaded TNT substrates. The coating was designed to release both the tethered gentamicin and the DFO encapsulated within the TNT upon cleavage by hyaluronidase, with the latter promoting osteogenesis and angiogenesis around the implant. *In vitro* cultures supported the antibacterial properties of the coating against *E. coli* and *S. aureus*, as well as the ability of the DFO-bearing coating to enhance the gene expression of osteogenic and angiogenic markers of rat bone marrow derived stromal cells. The *in vivo* performance of this coating in combating periprosthetic infections, however, was not evaluated. How hyaluronidases present in the host skeletal tissue environment may complicate the triggered release of antibiotics in these designs remains unaddressed.

We recently modified titanium surface using poly(ethylene glycol) dimethacrylate (PEGDMA) hydrogel to covalently attach vancomycin via an oligonucleotide linker sensitive to micrococcal nuclease (MN) of *S. aureus*. This design enabled the timely release of vancomycin in the presence of *S. aureus* to kill the bacteria both on the implant surface and within the periprosthetic tissue environment (Figure 6).<sup>21</sup> By inoculating 40-CFU bioluminescent Xen-29 *S. aureus* in murine femoral canals prior to the insertion of Ti6Al4V IM pins coated with PEGDMA-Oligo control hydrogel (without vancomycin), we showed that the infection was established at 2 days post-operation and sustained over the course of

21 days as shown by bioluminescence imaging (Figure 6a, bottom panel). By contrast, no obvious bioluminescence was seen from the femurs inserted with the IM pins coated with PEGDMA-Oligo-Vanco at any time point during the 21 day follow-up (Figure 6a, top panel), and the quantification of bioluminescent signals confirmed significant reduction in intensity by >95% at 2 days post-operation compared to the control groups (Figure 6b). Consistent with the longitudinal imaging data, no bacteria were recovered from the retrieved IM pins with the PEGDMA-Oligo-Vanco coating, supporting complete eradication of surface-bound bacteria, while >500 CFU *S. aureus* were recovered from the retrieved IM pins with the PEGDMA-Oligo control coating (Figure 6c). Finally,  $\mu$ CT imaging of femurs treated with IM pins coated with the PEGDMA-Oligo control hydrogel showed clear signs of osteolysis at 3 weeks post-operation while those receiving PEGDMA-Oligo-Vanco coated IM pins exhibited completely normal cortical bone morphology (Figure 6d). This promising bacterial enzyme-triggered release strategy is being further optimized to further enhance the stability of the nucleotide linker to mammalian nucleases.

**3.3.3. AMP releasing coatings**—AMPs have also been released from implant coatings as free-diffusing bactericidal agents. For example, Kazemzadeh-Narbat *et al.*<sup>184</sup> developed a multilayered coating consisting of TiO<sub>2</sub> nanotubes (TNTs), a thin layer of calcium phosphate, and a phospholipid film for sustained delivery of broad-spectrum AMP HHC-36 (KRWWKWRR-NH<sub>2</sub>). The AMP was impregnated in each layer while the lipid layer was designed as a membrane-mimicking barrier to prevent burst release of AMP while ensuring good cytocompatibility of the coating. The coating showed controlled and sustained release of the AMP over the course of a few days and was shown to inhibit the growth of both Gram-positive (*S. aureus*) and Gram-negative (*P. aeruginosa*) bacteria *in vitro*. Short-duration cell culture experiments (a few hours) showed good attachment of osteoblast-like cells MG-63, moderate platelet activation and adhesion, and low red blood cell lysis on the coated implant surface. Similarly, Shen *et al.*<sup>185</sup> used TNTs on titanium substrates to load AMP cecropin B and sealed them with multilayer coatings of chitosan/sodium hyaluronic-ecropin B. The *in vitro* release of the AMP from the coating could be triggered by exogenous hyaluronidase or the hyaluronidase secreted by *S. aureus*. The coating exhibited good bactericidal capacity against *S. aureus* and *S. epidermidis* over 72 h. For both coating systems and other similar strategies, however, more rigorous longer-term cytocompatibility evaluations with relevant primary cells (instead of immortalized cell lines), particularly as a function of the AMP release, and appropriate *in vivo* bactericidal efficacy and biocompatibility evaluations of the coating would be necessary to establish their translational potentials.

Overall, despite AMPs' bactericidal activities against both Gram-positive and Gram-negative bacteria, their applications have been limited by their *in vivo* instability and cytotoxicity.<sup>186, 187</sup> Several approaches have been introduced in the AMP therapeutics design and delivery to address these limitations without compromising their bactericidal potencies. For examples, Carmona *et al.*<sup>188</sup> used D-amino acids to synthesize AMPs which showed improved stability against trypsin digestion compared to those based on L-amino acids. Ron-Doitch *et al.*<sup>189</sup> used liposomes to encapsulate AMPs to reduce their cytotoxicity. Finally, AMPs have also been conjugated with antibodies for more targeted delivery to bacteria of

interest to reduce their systemic toxicity.<sup>190</sup> Successful outcomes of these approaches may inspire their implementations in the design of more effective and safer AMP-releasing implant coatings.

### 3.4 Coatings Responsive to Photothermal/Photodynamic Therapy

The photothermal therapy (PTT) and photodynamic therapy (PDT) based on near infrared (NIR) irradiation have gained increasing attention for a range of medical interventions from cancer therapy to infection mitigation because of their minimal invasiveness and regional selectivity. PTT utilizes photothermal agents to transform optical energy into local heat (hyperthermia) while PDT delivers treatment through photochemical reactions (e.g. generation of ROS) triggered by photosensitizers. PTT has also been explored to destroy bacteria or biofilm via local hyperthermia.<sup>191–194</sup> However, for the bactericidal efficacy to reach over 90%, local hyperthermia around 85 °C is required, which could cause significant tissue necrosis.<sup>195, 196</sup> Combining NIR-based PTT and PDT, moderate local hyperthermia and the *in situ* generated ROS known for destructive actions on bacterial proteins or DNA<sup>197, 198</sup> can be exploited to synergistically kill bacteria with reduced risk for tissue necrosis.

For example, Yuan *et al.*<sup>194</sup> developed a multifunctional hybrid coating on titanium for combating established biofilms by PTT/PDT with NIR activation. Specifically, mesoporous polydopamine nanoparticles were immobilized onto amino modified titanium surface, functionalized with integrin-binding peptide RGDC to improve cytocompatibility and then loaded with photosensitizer Indocyanine Green (ICG) via  $\pi$ - $\pi$  stacking. The functionalized surface reached a local temperature of ~50 °C after 300 s of NIR (808 nm) irradiation. Prior studies showed that local transient temperature increases should be kept below 70 °C to avoid potential skeletal tissue necrosis.<sup>199</sup> The combination of the moderate PTT at 50 °C with the ICG-based PDT improved the *in vitro* inhibition of initial *S. aureus* adhesion on the substrate to nearly 99.7% from the 63% achieved by the moderate PTT alone. Importantly, the combinatorial PTT/PDT therapy eradicated *S. aureus* biofilm pre-formed on the implant *in vivo* with an efficiency of 95%, with the NIR treated implant still exhibiting good osteointegration, supporting mitigated negative impact on surrounding tissue. Similarly, Li *et al.*<sup>200</sup> used red phosphorous (RP) and *in situ* generated peroxynitrite ( $\text{ONOO}^-$ ), an oxidizing agent lethal towards pathogens, to eradicate MRSA biofilm on titanium surfaces via PTT/PDT. Poly(vinyl alcohol), chitosan and polydopamine and nitric oxide (NO)-releasing S-nitrosuccinic acid (RSNO)-based hydrogel was used to coat and stabilize RP deposited on the titanium surface. Under NIR irradiation, the ROS reacted with the NO released from RSNO to generate peroxynitrite. The synergistic effects of hyperthermia, ROS and peroxynitrite led to the elimination of MRSA biofilm with a 93% efficiency *in vitro*. In addition, the *in vivo* results validated excellent biofilm eradication from the titanium surfaces under NIR irradiation without compromising osteogenesis, supporting the safety of the employed PTT/PDT strategy.



## 4. Conclusions and Future Direction

The number of bactericidal and anti-fouling surfaces that has been designed and explored for anti-infection applications is quickly expanding. This review provides an overview of the technical developments in the past 2 decades for these translational efforts. Anti-fouling and QS-interfering surfaces have been designed to reduce/inhibit bacterial adhesion, colonization and biofilm formation in the first place. Bactericidal surfaces engineered with topographical features or stably tethered antibiotics or AMPs have been shown to disrupt bacterial cells that come in direct contact with the surface. These strategies, however, do not protect surrounding tissues from infections. The combination of anti-fouling/bactericidal surface modification with on-demand release of freely diffusing antibacterial agents, triggered by the presence of bacteria within the periprosthetic tissue environment, is highly desirable as it may provide timely bacterial clearance without suboptimal release of local bactericidal agents that could cause drug resistance. For such a design to successfully translate to practical uses, however, greater consideration should be given to designing scalable coating systems that can efficiently sense and respond to the bacterial presence and release bactericidal agents in response to enzymatic activities unique to the pathogen while remain stable against non-specific cleavages by host enzymes. Meanwhile, combining surface modifications that discourages bacterial colonization/biofilm formation with appropriately timed systemic injections of conventional antibiotics has the potential to improve both the safety (due to reduced injection dose and/or duration) and efficacy (due to greater susceptibility of planktonic bacteria to antibiotics) of the latter. Finally, strategies for combating established biofilms, such as photodynamic therapy and local delivery of biofilm matrix-degrading enzymes or surface tension-reducing surfactants that induce biofilm dispersal,<sup>31</sup> may also find synergy with the anti-fouling/bactericidal surface modifications in discouraging the recolonization and survival of the remainder/dispersed bacteria. Overall, the need for multi-modality strategies<sup>32, 201, 202</sup> that take into account of various stages of pathogenesis and translational considerations (cost and scalability) while minimizing negative impact on periprosthetic host tissues or encouraging implant-tissue integrations are increasingly recognized.

To expedite clinical translations, novel implant surface modification strategies should be rigorously examined for both short-term and long-term efficacies in preventing or eradicating periprosthetic infections using suitable animal infection models that replicate clinically relevant scenarios, from the type and inoculation doses of bacteria, design and anatomical location of the implant, choice of animals, to the duration and outcome measures of the studies. A number of reviews over the past 2 decades on the pros and cons of common small (e.g. rodents) and large animal (e.g. rabbits, dogs) models and prosthesis designs for evaluating therapeutic strategies against periprosthetic orthopedic infections<sup>203–207</sup> will be of great values to such study designs. Other considerations include ensuring the cytocompatibility and biocompatibility of the implant surface modifications and the safety of the physical triggering methods (e.g. ultrasound, photo irradiation, hyperthermia) applied. These critical pre-clinical assessments will expedite the successful translation of these emerging implant surface modification strategies to combat PJI, not only significantly improving patients' well-being but making a positive social and economic impact.

## Acknowledgement

This work was supported by National Institutes of Health grants R01AR068418 and R01AR078044.

## References

1. Lynch AS; Robertson GT Bacterial and Fungal Biofilm Infections. In *Annu. Rev. Med* 2008; 415–428. [PubMed: 17937586]
2. Donlan RM Biofilm formation: A Clinically Relevant Microbiological Process. *Clin. Infect. Dis* 2001, 33 (8), 1387–1392. [PubMed: 11565080]
3. Darouiche RO Treatment of Infections Associated with Surgical Implants. *N. Engl. J. Med* 2004, 350 (14), 1422–1429. [PubMed: 15070792]
4. Schwarz EM; Parvizi J; Gehrke T; Aiyer A; Battenberg A; Brown SA; Callaghan JJ; Citak M; Egol K; Garrigues GE; Ghert M; Goswami K; Green A; Hammond S; Kates SL; McLaren AC; Mont MA; Namdari S; Obrebsky WT; O’Toole R; Raikin S; Restrepo C; Ricciardi B; Saeed K; Sanchez-Sotelo J; Shohat N; Tan T; Thirukumaran CP; Winters B, 2018 International Consensus Meeting on Musculoskeletal Infection: Research Priorities from the General Assembly Questions. *J. Orthop. Res* 2019, 37 (5), 997–1006. [PubMed: 30977537]
5. Francolini I; Vuotto C; Piozzi A; Donelli G Antifouling and Antimicrobial Biomaterials: an Overview. *APMIS* 2017, 125 (4), 392–417. [PubMed: 28407425]
6. Tande AJ; Patel R Prosthetic Joint Infection. *Clin. Microbiol. Rev* 2014, 27 (2), 302–345. [PubMed: 24696437]
7. Song Z; Borgwardt L; Høiby N; Wu H; Sørensen TS; Borgwardt A Prosthesis Infections after Orthopedic Joint Replacement: the Possible Role of Bacterial Biofilms. *Orthop. Rev. (Pavia)* 2013, 5 (2), 65–71. [PubMed: 23888204]
8. Yokogawa N; Ishikawa M; Nishitani K; Beck CA; Tsuchiya H; Mesfin A; Kates SL; Daiss JL; Xie C; Schwarz EM Immunotherapy Synergizes with Debridement and Antibiotic Therapy in a Murine 1-stage Exchange Model of MRSA Implant-associated Osteomyelitis. *J Orthop. Res* 2018, 36 (6), 1590–1598. [PubMed: 29405452]
9. Trampuz A; Widmer AF Infections Associated with Orthopedic Implants. *Curr. Opin. Infect. Dis* 2006, 19 (4), 349–356. [PubMed: 16804382]
10. Trampuz A; Zimmerli W Antimicrobial Agents in Orthopaedic Surgery: Prophylaxis and Treatment. *Drugs* 2006, 66 (8), 1089–1105. [PubMed: 16789794]
11. Zimmerli W; Widmer AF; Blatter M; Frei R; Ochsner PE Role of Rifampin for Treatment of Orthopedic Implant-related Staphylococcal Infections: a Randomized Controlled Trial. *Foreign-Body Infection (FBI) Study Group. JAMA* 1998, 279 (19), 1537–1541. [PubMed: 9605897]
12. Anagnostakos K; Schmid NV; Kelm J; Grün U; Jung J Classification of Hip Joint Infections. *Int. J. Med. Sci* 2009, 6 (5), 227–233. [PubMed: 19841729]
13. Orapiriyakul W; Young PS; Damiati L; Tsimbouri PM Antibacterial Surface Modification of Titanium Implants in Orthopaedics. In *J. Tissue Eng* 2018, 9, 2041731418789838. [PubMed: 30083308]
14. Puckett SD; Taylor E; Raimondo T; Webster TJ The Relationship Between the Nanostructure of Titanium Surfaces and Bacterial Attachment. *Biomaterials* 2010, 31 (4), 706–713. [PubMed: 19879645]
15. Moran E; Byren I; Atkins BL The Diagnosis and Management of Prosthetic Joint Infections. *J. Antimicrob. Chemother* 2010, 65, iii45–iii54. [PubMed: 20876628]
16. de Mesy Bentley KL; Trombetta R; Nishitani K; Bello-Irizarry SN; Ninomiya M; Zhang L; Chung HL; McGrath JL; Daiss JL; Awad HA; Kates SL; Schwarz EM Evidence of *Staphylococcus aureus* Deformation, Proliferation and Migration in Canaliculi of Live Cortical Bone in Murine Models of Osteomyelitis. *J. Bone Miner. Res* 2017, 32 (5), 985–990. [PubMed: 27933662]
17. Buchholz HW; Engelbrecht H [Depot Effects of Various Antibiotics Mixed with Palacos Resins]. *Chirurg* 1970, 41 (11), 511–515. [PubMed: 5487941]

18. Jose B; Antoci V; Zeiger AR; Wickstrom E; Hickok NJ Vancomycin Covalently Bonded to Titanium Beads Kills *Staphylococcus aureus*. *Chem. Biol* 2005, 12 (9), 1041–1048. [PubMed: 16183028]
19. Gerits E; Kucharikova S; Van Dijk P; Erdtmann M; Krona A; Lovenklev M; Frohlich M; Dovgan B; Impellizzeri F; Braem A; Vleugels J; Robijns SC; Steenackers HP; Vanderleyden J; De Brucker K; Thevissen K; Cammue BP; Fauvart M; Verstraeten N; Michiels J Antibacterial Activity of a New Broad-spectrum Antibiotic Covalently Bound to Titanium Surfaces. *J. Orthop. Res* 2016, 34 (12), 2191–2198. [PubMed: 27003909]
20. Berger RA; Jacobs JJ; Quigley LR; Rosenberg AG; Galante JO Primary Cementless Acetabular Reconstruction in Patients Younger than 50 Years Old. 7- to 11-year results. *Clin. Orthop. Relat. Res* 1997, 344, 216–226.
21. Ghimire A; Skelly JD; Song J, Micrococcal-Nuclease-Triggered On-Demand Release of Vancomycin from Intramedullary Implant Coating Eradicates *Staphylococcus aureus* Infection in Mouse Femoral Canals. *ACS Cent. Sci* 2019, 5 (12), 1929–1936. [PubMed: 31893222]
22. Zhang B; Braun BM; Skelly JD; Ayers DC; Song J, Significant Suppression of *Staphylococcus aureus* Colonization on Intramedullary Ti6Al4V Implants Surface-Grafted with Vancomycin-Bearing Polymer Brushes. *ACS Appl. Mater. Interfaces* 2019, 11 (32), 28641–28647. [PubMed: 31313901]
23. Shivapooja P; Wang Q; Orihuela B; Rittschof D; López GP; Zhao X, Bioinspired Surfaces with Dynamic Topography for Active Control of Biofouling. *Adv. Mater* 2013, 25 (10), 1430–1434. [PubMed: 23292960]
24. Su Y; Zhi Z; Gao Q; Xie M; Yu M; Lei B; Li P; Ma PX, Autoclaving-Derived Surface Coating with In Vitro and In Vivo Antimicrobial and Antibiofilm Efficacies. *Adv. Healthcare Mater* 2017, 6 (6), 1601173.
25. Li J; Tan L; Liu X; Cui Z; Yang X; Yeung KWK; Chu PK; Wu S, Balancing Bacteria–Osteoblast Competition through Selective Physical Puncture and Biofunctionalization of ZnO/Polydopamine/Arginine-Glycine-Aspartic Acid-Cysteine Nanorods. *ACS Nano* 2017, 11 (11), 11250–11263. [PubMed: 29049874]
26. Ivanova EP; Truong VK; Webb HK; Baulin VA; Wang JY; Mohammadi N; Wang F; Fluke C; Crawford RJ Differential Attraction and Repulsion of *Staphylococcus aureus* and *Pseudomonas aeruginosa* on Molecularly Smooth Titanium Films. *Sci. Rep* 2011, 1 (1), 165. [PubMed: 22355680]
27. Mrabet B; Nguyen MN; Majbri A; Mahouche S; Turmine M; Bakhrouf A; Chehimi MM Anti-fouling Poly(2-hydroxyethyl methacrylate) Surface Coatings with Specific Bacteria Recognition Capabilities. *Surf. Sci* 2009, 603 (16), 2422–2429.
28. Lichter JA; Thompson MT; Delgadillo M; Nishikawa T; Rubner MF; Van Vliet KJ, Substrata Mechanical Stiffness Can Regulate Adhesion of Viable Bacteria. *Biomacromolecules* 2008, 9 (6), 1571–1578. [PubMed: 18452330]
29. Yang H; Jia B; Zhang Z; Qu X; Li G; Lin W; Zhu D; Dai K; Zheng Y Alloying Design of Biodegradable Zinc as Promising Bone Implants for Load-bearing Applications. *Nat. Commun* 2020, 11 (1), 401. [PubMed: 31964879]
30. Arciola CR; Campoccia D; Montanaro L, Implant Infections: Adhesion, Biofilm Formation and Immune Evasion. *Nat. Rev. Microbiol* 2018, 16 (7), 397–409. [PubMed: 29720707]
31. Guillhen C; Forestier C; Balestrino D, Biofilm Dispersal: Multiple Elaborate Strategies for Dissemination of Dacteria with Unique Properties. *Mol. Microbiol* 2017, 105 (2), 188–210. [PubMed: 28422332]
32. Fischer NG; Munchow EA; Tamerler C; Bottino MC; Aparicio C, Harnessing Biomolecules for Bioinspired Dental Biomaterials. *J. Mater. Chem. B* 2020, 8 (38), 8713–8747. [PubMed: 32747882]
33. Orapiriyakul W; Young PS; Damiati L; Tsimbouri PM, Antibacterial Surface Modification of Titanium Implants in Orthopaedics. *J. Tissue. Eng* 2018, 9, 2041731418789838. [PubMed: 30083308]

34. Chouirfa H; Bouloussa H; Migonney V; Falentin-Daudre C, Review of Titanium Surface Modification Techniques and Coatings for Antibacterial Applications. *Acta. Biomater* 2019, 83, 37–54. [PubMed: 30541702]
35. Quinn J; McFadden R; Chan CW; Carson L, Titanium for Orthopedic Applications: An Overview of Surface Modification to Improve Biocompatibility and Prevent Bacterial Biofilm Formation. *iScience* 2020, 23 (11), 101745. [PubMed: 33235984]
36. Teughels W; Van Assche N; Sliepen I; Quirynen M Effect of Material Characteristics and/or Surface Topography on Biofilm Development. *Clin. Oral Implants Res* 2006, 17 Suppl 2, 68–81. [PubMed: 16968383]
37. Park KD; Kim YS; Han DK; Kim YH; Lee EHB; Suh H; Choi KS Bacterial Adhesion on PEG Modified Polyurethane Surfaces. *Biomaterials* 1998, 19 (7), 851–859. [PubMed: 9663762]
38. Albrektsson T; Wennerberg A Oral implant surfaces: Part I--Review Focusing on Topographic and Chemical Properties of Different Surfaces and In Vivo Responses to Them. *Int. J. Prosthodont* 2004, 17 (5), 536–543. [PubMed: 15543910]
39. Scheuerman TR; Camper AK; Hamilton MA Effects of Substratum Topography on Bacterial Adhesion. *J. Colloid Interface Sci* 1998, 208 (1), 23–33. [PubMed: 9820746]
40. Damodaran VB; Murthy NS, Bio-Inspired Strategies for Designing Antifouling Biomaterials. *Biomater. Res* 2016, 20 (1), 18. [PubMed: 27326371]
41. Xie M; Wang Y; Zhao W, Design Novel Three-dimensional Network Nanostructure for Lubricant Infused on Titanium Alloys Towards Long-term Anti-fouling. *Colloids Surf. B: Biointerfaces* 2021, 197, 111375. [PubMed: 33011501]
42. Hizal F; Rungraeng N; Lee J; Jun S; Busscher HJ; van der Mei HC; Choi C-H, Nanoengineered Superhydrophobic Surfaces of Aluminum with Extremely Low Bacterial Adhesivity. *ACS Appl. Mater. Interfaces* 2017, 9 (13), 12118–12129. [PubMed: 28291321]
43. Gallardo-Moreno AM; Pacha-Olivenza MA; Saldaña L; Pérez-Giraldo C; Bruque JM; Vilaboa N; González-Martín ML In Vitro Biocompatibility and Bacterial Adhesion of Physico-chemically Modified Ti6Al4V Surface by Means of UV Irradiation. *Acta Biomater* 2009, 5 (1), 181–192. [PubMed: 18768375]
44. Gottenbos B; van der Mei HC; Klatter F; Grijpma DW; Feijen J; Nieuwenhuis P; Busscher HJ Positively Charged Biomaterials Exert Antimicrobial Effects on Gram-negative Bacilli in Rats. *Biomaterials* 2003, 24 (16), 2707–2710. [PubMed: 12711516]
45. Li Z; Guo Z Bioinspired Surfaces with Wettability for Antifouling Application. *Nanoscale* 2019, 11 (47), 22636–22663. [PubMed: 31755511]
46. Nouri A; Wen C 1 - Introduction to Surface Coating and Modification for Metallic Biomaterials. In *Surface Coating and Modification of Metallic Biomaterials*; Wen C, Ed.; Woodhead Publishing: 2015; pp 3–60.
47. Ludecke C; Roth M; Yu W; Horn U; Bossert J; Jandt KD Nanorough Titanium Surfaces Reduce Adhesion of Escherichia coli and Staphylococcus aureus Via Nano Adhesion Points. *Colloids Surf. B Biointerfaces* 2016, 145, 617–625. [PubMed: 27288816]
48. Song R; Zhang Y; Huang Q; Yang Y; Lin L; Liang J; Hu R; Rui G; Lin C Facile Construction of Structural Gradient of TiO<sub>2</sub> Nanotube Arrays on Medical Titanium for High Throughput Evaluation of Biocompatibility and Antibacterial Property. *ACS Appl. Bio Mater* 2018, 1 (4), 1056–1065.
49. Cheng YF; Mei YH; Sathishkumar G; Lu ZS; Li CM; Wang F; Xia QY; Xu LQ Tannic Acid-assisted Deposition of Silk Sericin on the Titanium Surfaces for Antifouling Application. *Colloid Interface Sci. Commun* 2020, 35, 100241.
50. Francolini I; Donelli G; Vuotto C; Baroncini FA; Stoodley P; Taresco V; Martinelli A; D'Ilario L; Piozzi A Antifouling Polyurethanes to Fight Device-related Staphylococcal Infections: Synthesis, Characterization, and Antibiofilm Efficacy. *Pathog. Dis* 2014, 70 (3), 401–407. [PubMed: 24532590]
51. Francolini I; Crisante F; Martinelli A; D'Ilario L; Piozzi A Synthesis of Biomimetic Segmented Polyurethanes as Antifouling Biomaterials. *Acta Biomater* 2012, 8 (2), 549–558. [PubMed: 22051237]

52. Zhang X; Wang L; Levänen E Superhydrophobic Surfaces for the Reduction of Bacterial Adhesion. *RSC Adv* 2013, 3 (30), 12003–12020.
53. Braem A; Van Mellaert L; Hofmans D; De Waelheyns E; Anné J; Schrooten J; Vleugels J Bacterial Colonisation of Porous Titanium Coatings for Orthopaedic Implant Applications – Effect of Surface Roughness and Porosity. *Powder Metall* 2013, 56 (4), 267–271.
54. Scardino AJ; Guenther J; de Nys R Attachment Point Theory Revisited: the Fouling Response to a Microtextured Matrix. *Biofouling* 2008, 24 (1), 45–53. [PubMed: 18066730]
55. Barthlott W; Neinhuis C Purity of the Sacred Lotus, or Escape from Contamination in Biological Surfaces. *Planta* 1997, 202 (1), 1–8.
56. Zhang Y-L; Xia H; Kim E; Sun H-B Recent Developments in Superhydrophobic Surfaces with Unique Structural and Functional Properties. *Soft Matter* 2012, 8 (44), 11217–11231.
57. Zhang X; Shi F; Niu J; Jiang Y; Wang Z Superhydrophobic Surfaces: From Structural Control to Functional Application. *J. Mater. Chem* 2008, 18 (6), 621–633.
58. Fadeeva E; Truong VK; Stiesch M; Chichkov BN; Crawford RJ; Wang J; Ivanova EP Bacterial Retention on Superhydrophobic Titanium Surfaces Fabricated by Femtosecond Laser Ablation. *Langmuir* 2011, 27 (6), 3012–3019. [PubMed: 21288031]
59. Tang Peifu, Z. W, Wang Yan, Zhang Boxun, Wang Hao.; Lin Changjian, Z. a. L. Effect of Superhydrophobic Surface of Titanium on Staphylococcus aureus Adhesion. *J. Nanomater* 2011, 2011.
60. Huang Q; Lin L; Yang Y; Hu R; Vogler EA; Lin C Role of Trapped air in the Formation of Cell-and-Protein Micropatterns on Superhydrophobic/Superhydrophilic Microtemplated Surfaces. *Biomaterials* 2012, 33 (33), 8213–8220. [PubMed: 22917736]
61. Ostuni E; Chapman RG; Liang MN; Meluleni G; Pier G; Ingber DE; Whitesides GM Self-Assembled Monolayers That Resist the Adsorption of Proteins and the Adhesion of Bacterial and Mammalian Cells. *Langmuir* 2001, 17 (20), 6336–6343.
62. Kingshott P; Wei J; Bagge-Ravn D; Gadegaard N; Gram L Covalent Attachment of Poly(ethylene glycol) to Surfaces, Critical for Reducing Bacterial Adhesion. *Langmuir* 2003, 19 (17), 6912–6921.
63. Tedjo C; Neoh KG; Kang ET; Fang N; Chan V Bacteria–Surface Interaction in the Presence of Proteins and Surface Attached Poly(ethylene glycol) Methacrylate Chains. *J. Biomed. Mater. Res. A* 2007, 82 (2), 479–491. [PubMed: 17295255]
64. Lee HJ; Park KD; Park HD; Lee WK; Han DK; Kim SH; Kim YH Platelet and Bacterial Repellence on Sulfonated Poly(ethylene glycol)-acrylate Copolymer Surfaces. *Colloids Surf. B: Biointerfaces* 2000, 18 (3), 355–370. [PubMed: 10915957]
65. Saldarriaga Fernández IC; van der Mei HC; Lochhead MJ; Grainger DW; Busscher HJ The Inhibition of the Adhesion of Clinically Isolated Bacterial Strains on Multi-Component Cross-Linked Poly(ethylene glycol)-based Polymer Coatings. *Biomaterials* 2007, 28 (28), 4105–4112. [PubMed: 17573108]
66. Zoulalian V; Zürcher S; Tosatti S; Textor M; Monge S; Robin J-J, Self-Assembly of Poly(ethylene glycol)–Poly(alkyl phosphonate) Terpolymers on Titanium Oxide Surfaces: Synthesis, Interface Characterization, Investigation of Nonfouling Properties, and Long-Term Stability. *Langmuir* 2010, 26 (1), 74–82. [PubMed: 19691273]
67. Schlenoff JB, Zwitteration: Coating Surfaces with Zwitterionic Functionality to Reduce Nonspecific Adsorption. *Langmuir* 2014, 30 (32), 9625–9636. [PubMed: 24754399]
68. Krishnan S; Weinman CJ; Ober CK Advances in Polymers for Anti-Biofouling Surfaces. *J. Mater. Chem* 2008, 18 (29), 3405–3413.
69. Mishra S; Horswill AR, Heparin Mimics Extracellular DNA in Binding to Cell Surface-Localized Proteins and Promoting Staphylococcus aureus Biofilm Formation. *mSphere* 2017, 2 (3), e00135–17. [PubMed: 28656173]
70. Maan AMC; Hofman AH; de Vos WM; Kamperman M, Recent Developments and Practical Feasibility of Polymer-Based Antifouling Coatings. *Adv. Funct. Mater* 2020, 30 (32), 2000936.
71. Mas-Moruno C; Su B; Dalby MJ, Multifunctional Coatings and Nanotopographies: Toward Cell Instructive and Antibacterial Implants. *Adv. Healthcare Mater* 2019, 8 (1), 1801103.

72. Lüsse S; Arnold K, The Interaction of Poly(ethylene glycol) with Water Studied by <sup>1</sup>H and <sup>2</sup>H NMR Relaxation Time Measurements. *Macromolecules* 1996, 29 (12), 4251–4257.
73. Oesterhelt F; Rief M; Gaub HE Single Molecule Force Spectroscopy by AFM Indicates Helical Structure of Poly(ethylene-glycol) in Water. *New J. Phys* 1999, 1, 6–6.
74. Aray Y; Marquez M; Rodríguez J; Vega D; Simón-Manso Y; Coll S; Gonzalez C; Weitz DA, Electrostatics for Exploring the Nature of the Hydrogen Bonding in Polyethylene Oxide Hydration. *J. Phys. Chem. B* 2004, 108 (7), 2418–2424.
75. Chen S; Li L; Zhao C; Zheng J Surface Hydration: Principles and Applications Toward Low-Fouling/Nonfouling Biomaterials. *Polymer* 2010, 51 (23), 5283–5293.
76. Khoo X; Hamilton P; O'Toole GA; Snyder BD; Kenan DJ; Grinstaff MW, Directed Assembly of PEGylated-Peptide Coatings for Infection-Resistant Titanium Metal. *J. Am. Chem. Soc* 2009, 131 (31), 10992–10997. [PubMed: 19621876]
77. Buxadera-Palmero J; Calvo C; Torrent-Camarero S; Gil FJ; Mas-Moruno C; Canal C; Rodríguez D Biofunctional Polyethylene Glycol Coatings on Titanium: An In Vitro-Based Comparison of Functionalization Methods. *Colloids Surf. B: Biointerfaces* 2017, 152, 367–375. [PubMed: 28135680]
78. Herold DA; Keil K; Bruns DE Oxidation of Polyethylene Glycols by Alcohol Dehydrogenase. *Biochem. Pharmacol* 1989, 38 (1), 73–76. [PubMed: 2642704]
79. Ratner BD Reducing Capsular Thickness and Enhancing Angiogenesis around Implant Drug Release Systems. *J. Control. Release* 2002, 78 (1), 211–218. [PubMed: 11772462]
80. Crouzet C; Decker C; Marchal J Caractérisation de Réactions Primaires de Dégradation Oxydante au Cours de L'autoxydation des Poly(oxyéthylène)s à 25°C: Étude en Solution Aqueuse avec Amorçage par Radiolyse du Solvant, 8. Étude cinétique en fonction du ph compris entre 1 et 13. *Die Makromolekulare Chemie* 1976, 177 (1), 145–157.
81. Gerhardt W; Martens C, Zur Oxydation von Polyethylenoxiden und Polyethylenoxidethern; Die Bildung von Acetaldehyd bei der Oxydation von Diethylenglycol mit Sauerstoff. *Zeitschrift für Chemie* 1985, 25 (4), 143–143.
82. Zwaal RFA; Comfurius P; Van Deenen LLM Membrane Asymmetry and Blood Coagulation. *Nature* 1977, 268 (5618), 358–360. [PubMed: 887167]
83. Zwaal RFA; Schroit AJ, Pathophysiologic Implications of Membrane Phospholipid Asymmetry in Blood Cells. *Blood* 1997, 89 (4), 1121–1132. [PubMed: 9028933]
84. Lewis AL Phosphorylcholine-Based Polymers and Their use in the Prevention of Biofouling. *Colloids Surf. B: Biointerfaces* 2000, 18 (3), 261–275. [PubMed: 10915948]
85. Hall B; le E Bird R; Kojima M; Chapman D Biomembranes as Models for Polymer Surfaces: V. Thrombelastographic Studies of Polymeric Lipids and Polyesters. *Biomaterials* 1989, 10 (4), 219–224. [PubMed: 2525934]
86. Hayward JA; Durrani AA; Shelton CJ; Lee DC; Chapman D Biomembranes as Models for Polymer Surfaces: III. Characterization of a Phosphorylcholine Surface Covalently Bound to Glass. *Biomaterials* 1986, 7 (2), 126–131. [PubMed: 3708064]
87. Ishihara K; Fukumoto K; Iwasaki Y; Nakabayashi N Modification of Polysulfone with Phospholipid Polymer for Improvement of the Blood Compatibility. Part 1. Surface Characterization. *Biomaterials* 1999, 20 (17), 1545–1551. [PubMed: 10482408]
88. Liu H; Liu L; Jiang X; Fan J; Peng W; Liu P; Yang T; Chen H; Jiang W; Yin G; Liu P; Shen J Rational Design of a Zwitterionic–Phosphonic Copolymer for the Surface Antifouling Modification of Multiple Biomedical Metals. *J. Mater. Chem. B* 2019, 7 (25), 4055–4065.
89. Cheng G; Zhang Z; Chen S; Bryers JD; Jiang S Inhibition of Bacterial Adhesion and Biofilm Formation on Zwitterionic Surfaces. *Biomaterials* 2007, 28 (29), 4192–4199. [PubMed: 17604099]
90. Liu PS; Domingue E; Ayers DC; Song J, Modification of Ti6Al4V Substrates with Well-defined Zwitterionic Polysulfobetaine Brushes for Improved Surface Mineralization. *ACS Appl. Mater. Interfaces* 2014, 6 (10), 7141–7152. [PubMed: 24828749]
91. Liu P; Emmons E; Song J, A Comparative Study of Zwitterionic Ligands-mediated Biomaterialization and the Potential of Mineralized Zwitterionic Matrices for Bone Tissue Engineering. *J. Mater. Chem. B* 2014, 2 (43), 7524–7533. [PubMed: 25558374]

92. Liu P; Song J, Sulfobetaine as a Zwitterionic Mediator for 3D Hydroxyapatite Mineralization. *Biomaterials* 2013, 34 (10), 2442–2454. [PubMed: 23332320]
93. Zhang B; Skelly JD; Braun BM; Ayers DC; Song J Surface-Grafted Zwitterionic Polymers Improve the Efficacy of a Single Antibiotic Injection in Suppressing *Staphylococcus aureus* Periprosthetic Infections. *ACS Appl. Bio Mater* 2020, 3, 5896–5904.
94. Fuqua WC; Winans SC; Greenberg EP Quorum Sensing in Bacteria: The LuxR-LuxI Family of Cell Density-Responsive Transcriptional Regulators. *J. Bacteriol* 1994, 176 (2), 269. [PubMed: 8288518]
95. Waters CM; Bassler BL QUORUM SENSING: Cell-to-Cell Communication in Bacteria. *Annu Rev. Cell Dev. Biol* 2005, 21 (1), 319–346. [PubMed: 16212498]
96. Niu C; Afre S; Gilbert ES Subinhibitory Concentrations of Cinnamaldehyde Interfere with Quorum Sensing. *Lett. Appl. Microbiol* 2006, 43 (5), 489–494. [PubMed: 17032221]
97. Topa SH; Palombo EA; Kingshott P; Blackall LL, Activity of Cinnamaldehyde on Quorum Sensing and Biofilm Susceptibility to Antibiotics in *Pseudomonas aeruginosa*. *Microorganisms* 2020, 8 (3), 455.
98. Brackman G; Breyne K; De Rycke R; Vermote A; Van Nieuwerburgh F; Meyer E; Van Calenbergh S; Coenye T, The Quorum Sensing Inhibitor Hamamelitannin Increases Antibiotic Susceptibility of *Staphylococcus aureus* Biofilms by Affecting Peptidoglycan Biosynthesis and eDNA Release. *Sci. Rep* 2016, 6 (1), 20321. [PubMed: 26828772]
99. Luo J; Dong B; Wang K; Cai S; Liu T; Cheng X; Lei D; Chen Y; Li Y; Kong J; Chen Y Baicalin Inhibits Biofilm Formation, Attenuates the Quorum Sensing-Controlled Virulence and Enhances *Pseudomonas aeruginosa* Clearance in a Mouse Peritoneal Implant Infection Model. *PLoS One* 2017, 12 (4), e0176883–e0176883. [PubMed: 28453568]
100. He Z; Wang Q; Hu Y; Liang J; Jiang Y; Ma R; Tang Z; Huang Z Use of the Quorum Sensing Inhibitor Furanone C-30 to Interfere with Biofilm Formation by *Streptococcus Mutans* and its luxS Mutant Strain. *Int. J. Antimicrob. Agents* 2012, 40 (1), 30–35. [PubMed: 22578766]
101. Kang M; Kim S; Kim H; Song Y; Jung D; Kang S; Seo J-H; Nam S; Lee Y, Calcium-Binding Polymer-Coated Poly(lactide-co-glycolide) Microparticles for Sustained Release of Quorum Sensing Inhibitors to Prevent Biofilm Formation on Hydroxyapatite Surfaces. *ACS Appl. Mater. Interfaces* 2019, 11 (8), 7686–7694. [PubMed: 30768237]
102. Mooney JA; Pridgen EM; Manasherob R; Suh G; Blackwell HE; Barron AE; Bollyky PL; Goodman SB; Amanatullah DF Periprosthetic Bacterial Biofilm and Quorum Sensing. *J. Orthop. Res* 2018, 36 (9), 2331–2339. [PubMed: 29663554]
103. Ivanova EP; Hasan J; Webb HK; Truong VK; Watson GS; Watson JA; Baulin VA; Pogodin S; Wang JY; Tobin MJ; Lobb C; Crawford RJ, Natural Bactericidal Surfaces: Mechanical Rupture of *Pseudomonas aeruginosa* Cells by Cicada Wings. *Small* 2012, 8 (16), 2489–2494. [PubMed: 22674670]
104. Kelleher SM; Habimana O; Lawler J; O’ Reilly B; Daniels S; Casey E; Cowley A Cicada Wing Surface Topography: An Investigation into the Bactericidal Properties of Nanostructural Features. *ACS Appl. Mater. Interfaces* 2016, 8 (24), 14966–14974. [PubMed: 26551558]
105. Hasan J; Jain S; Chatterjee K Nanoscale Topography on Black Titanium Imparts Multi-bifunctional Properties for Orthopedic Applications. *Sci. Rep* 2017, 7 (1), 41118. [PubMed: 28112235]
106. Wandiyanto JV; Cheeseman S; Truong VK; Kobaisi MA; Bizet C; Juodkazis S; Thissen H; Crawford RJ; Ivanova EP Outsmarting superbugs: Bactericidal Activity of Nanostructured Titanium Surfaces Against Methicillin- and Gentamicin-resistant *Staphylococcus aureus* ATCC 33592. *J. Mater. Chem. B* 2019, 7 (28), 4424–4431.
107. Diu T; Faruqi N; Sjoström T; Lamarre B; Jenkison HF; Su B; Ryadnov MG Cicada-Inspired Cell-instructive Nanopatterned Arrays. *Sci. Rep* 2014, 4, 7122. [PubMed: 25409910]
108. Bhadra CM; Khanh Truong V; Pham VTH; Al Kobaisi M; Seniutinas G; Wang JY; Juodkazis S; Crawford RJ; Ivanova EP Antibacterial Titanium Nano-patterned Arrays Inspired by Dragonfly Wings. *Sci. Rep* 2015, 5 (1), 16817. [PubMed: 26576662]

109. Cao Y; Su B; Chinnaraj S; Jana S; Bowen L; Charlton S; Duan P; Jakubovics NS; Chen J Nanostructured Titanium Surfaces Exhibit Recalcitrance Towards Staphylococcus epidermidis Biofilm Formation. *Sci. Rep* 2018, 8 (1), 1071. [PubMed: 29348582]
110. Jaggessar A; Mathew A; Wang H; Tesfamichael T; Yan C; Yarlagadda PKDV Mechanical, Bactericidal and Osteogenic Behaviours of Hydrothermally Synthesised TiO<sub>2</sub> Nanowire Arrays. *J. Mech. Behav. Biomed. Mater* 2018, 80, 311–319. [PubMed: 29459290]
111. Sengstock C; Lopain M; Motemani Y; Borgmann A; Khare C; Buenconsejo PJS; Schildhauer TA; Ludwig A; Koller M Structure-Related Antibacterial Activity of a Titanium Nanostructured Surface Fabricated by Glancing Angle Sputter Deposition. *Nanotechnol* 2014, 25.
112. Sjöström T; Nobbs AH; Su B Bactericidal Nanospine Surfaces via Thermal Oxidation of Ti Alloy Substrates. *Mater. Lett* 2016, 167, 22–26.
113. Pogodin S; Hasan J; Baulin VA; Webb HK; Truong VK; Nguyen HP; Boshkoviki V; Fluke CJ; Watson GS; Watson JA; Crawford RJ; Ivanova EP Biophysical Model of Bacterial Cell Interactions with Nanopatterned Cicada wing Surfaces. *Biophys. J* 2013, 104, 835–840. [PubMed: 23442962]
114. Fraioli R; Tsimbouri PM; Fisher LE; Nobbs AH; Su B; Neubauer S; Rechenmacher F; Kessler H; Ginebra M-P; Dalby MJ; Manero JM; Mas-Moruno C, Towards the Cell-instructive Bactericidal Substrate: Exploring the Combination of Nanotopographical Features and Integrin Selective Synthetic Ligands. *Sci. Rep* 2017, 7 (1), 16363. [PubMed: 29180787]
115. Tiller JC; Liao C-J; Lewis K; Klibanov AM Designing Surfaces that kill Bacteria on Contact. *PNAS* 2001, 98 (11), 5981–5985. [PubMed: 11353851]
116. Lewis K; Klibanov AM Surpassing Nature: Rational Design of Sterile-Surface Materials. *Trends Biotechnol* 2005, 23 (7), 343–348. [PubMed: 15922467]
117. Edupuganti OP; Antoci V Jr.; King SB; Jose B; Adams CS; Parvizi J; Shapiro IM; Zeiger AR; Hickok NJ; Wickstrom E Covalent Bonding of Vancomycin to Ti6Al4V Alloy Pins Provides long-term Inhibition of Staphylococcus aureus Colonization. *Bioorg. Med. Chem. Lett* 2007, 17 (10), 2692–2696. [PubMed: 17369042]
118. Antoci V Jr.; Adams CS; Hickok NJ; Shapiro IM; Parvizi J Vancomycin Bound to Ti Rods Reduces Periprosthetic Infection: Preliminary Study. *Clin. Orthop. Relat. Res* 2007, 461, 88–95. [PubMed: 17549034]
119. Zeng Q; Zhu Y; Yu B; Sun Y; Ding X; Xu C; Wu Y-W; Tang Z; Xu F-J Antimicrobial and Antifouling Polymeric Agents for Surface Functionalization of Medical Implants. *Biomacromolecules* 2018, 19 (7), 2805–2811. [PubMed: 29727575]
120. Ageitos JM; Sánchez-Pérez A; Calo-Mata P; Villa TG, Antimicrobial Peptides (AMPs): Ancient Compounds that Represent Novel Weapons in the Fight Against Bacteria. *Biochem. J Pharmacol* 2017, 133, 117–138.
121. Chen J; Zhu Y; Xiong M; Hu G; Zhan J; Li T; Wang L; Wang Y, Antimicrobial Titanium Surface via Click-Immobilization of Peptide and Its in Vitro/Vivo Activity. *ACS Biomater. Sci. Eng* 2019, 5 (2), 1034–1044.
122. Godoy-Gallardo M; Mas-Moruno C; Yu K; Manero JM; Gil FJ; Kizhakkedathu JN; Rodriguez D, Antibacterial Properties of hLfl-11 Peptide onto Titanium Surfaces: A Comparison Study Between Silanization and Surface Initiated Polymerization. *Biomacromolecules* 2015, 16 (2), 483–496. [PubMed: 25545728]
123. Langer R, New Methods of Drug Delivery. *Science* 1990, 249 (4976), 1527–1533. [PubMed: 2218494]
124. Dash A; Cudworth G Therapeutic Applications of Implantable Drug Delivery Systems. *J. Pharmacol. Toxicol. Methods* 1998, 40 (1), 1–12. [PubMed: 9920528]
125. Kumar A; Pillai J Chapter 13 - Implantable Drug Delivery Systems: An Overview. In *Nanostructures for the Engineering of Cells, Tissues and Organs*; Grumezescu AM, Ed.; William Andrew Publishing: 2018; pp 473–511.
126. Simchi A; Tamjid E; Pishbin F; Boccaccini AR Recent Progress in Inorganic and Composite Coatings with Bactericidal Capability for Orthopaedic Applications. *Nanomedicine*, 2011, 7 (1), 22–39. [PubMed: 21050895]



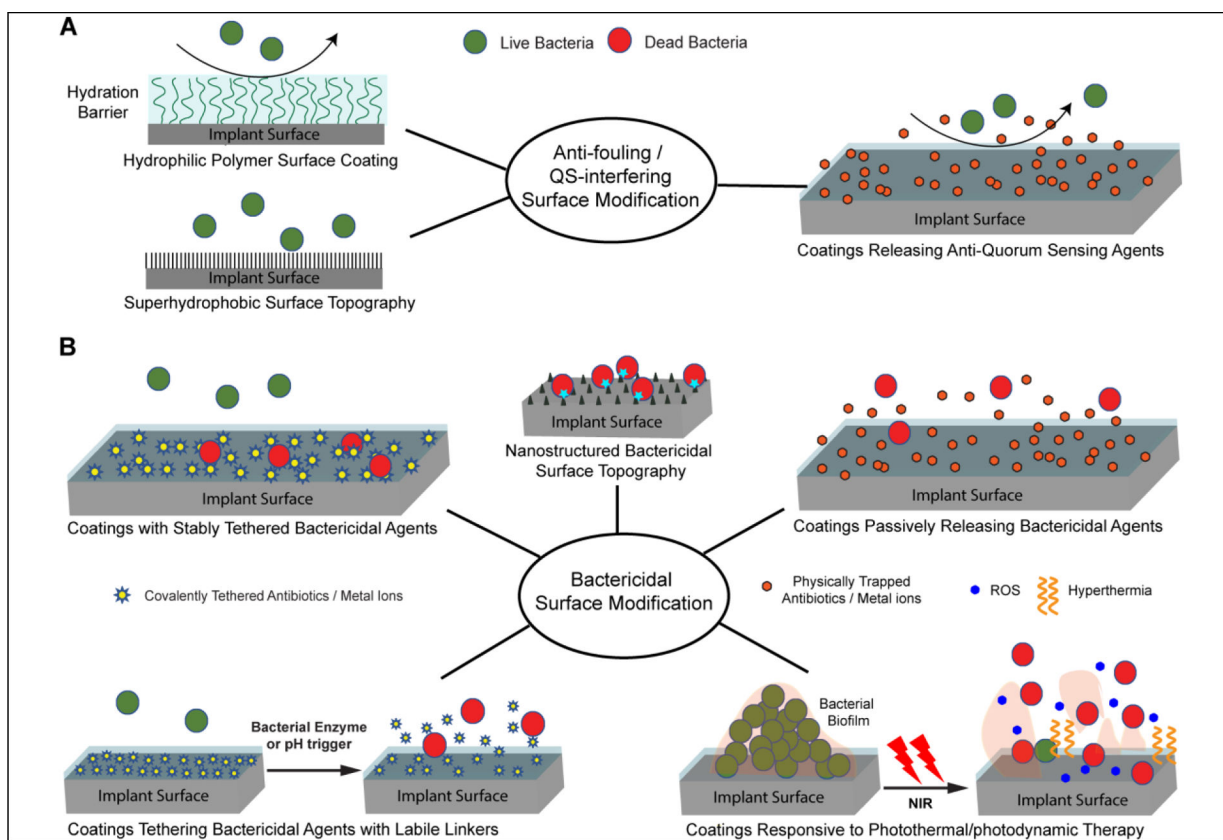
127. Lansdown AB Silver. I: Its Antibacterial Properties and Mechanism of Action. *J. Wound Care* 2002, 11 (4), 125–130. [PubMed: 11998592]
128. Klasen HJ Historical Review of the Use of Silver in the Treatment of Burns. I. Early Uses. *Burns* 2000, 26 (2), 117–130. [PubMed: 10716354]
129. Chopra I The Increasing Use of Silver-based Products as Antimicrobial Agents: a Useful Development or a Cause for Concern? *J. Antimicrob. Chemother* 2007, 59 (4), 587–590. [PubMed: 17307768]
130. Moore SL; Payne DN Types of Antimicrobial Agents. In Russell, Hugo & Ayliffe's Principles and Practice of Disinfection, Preservation & Sterilization, 2004, pp 8–97.
131. Moyer CA; Brebano L; Gravens DL; Margraf HW; Monafa WW Jr. Treatment of Large Human Burns With 0.5% Silver Nitrate Solution. *Arch. Surg* 1965, 90 (6), 812–867. [PubMed: 14333527]
132. Castellano JJ; Shafii SM; Ko F; Donate G; Wright TE; Mannari RJ; Payne WG; Smith DJ; Robson MC Comparative Evaluation of Silver-Containing Antimicrobial Dressings and Drugs. *Int. Wound J* 2007, 4 (2), 114–122. [PubMed: 17651227]
133. Amin Yavari S; Loozen L; Paganelli FL; Bakhshandeh S; Lietaert K; Groot JA; Fluit AC; Boel CHE; Alblas J; Vogely HC; Weinans H; Zadpoor AA Antibacterial Behavior of Additively Manufactured Porous Titanium with Nanotubular Surfaces Releasing Silver Ions. *ACS Appl. Mater. Interfaces* 2016, 8 (27), 17080–17089. [PubMed: 27300485]
134. Li M; Wang Y; Gao L; Sun Y; Wang J; Qu S; Duan K; Weng J; Feng B Porous Titanium Scaffold Surfaces Modified with Silver Loaded Gelatin Microspheres and Their Antibacterial Behavior. *Surf. Coat. Technol* 2016, 286, 140–147.
135. Dalecki AG; Haeili M; Shah S; Speer A; Niederweis M; Kutsch O; Wolschendorf F, Disulfiram and Copper Ions Kill *Mycobacterium tuberculosis* in a Synergistic Manner. *Antimicrob. Agents Chemother* 2015, 59 (8), 4835–4844. [PubMed: 26033731]
136. Faúndez G; Troncoso M; Navarrete P; Figueroa G, Antimicrobial Activity of Copper Surfaces Against Suspensions of Salmonella enterica and Campylobacter jejuni. *BMC Microbiol* 2004, 4 (1), 19. [PubMed: 15119960]
137. Wu C; Zhou Y; Xu M; Han P; Chen L; Chang J; Xiao Y, Copper-Containing Mesoporous Bioactive Glass Scaffolds with Multifunctional Properties of Angiogenesis Capacity, Osteostimulation and Antibacterial Activity. *Biomaterials* 2013, 34 (2), 422–433. [PubMed: 23083929]
138. Gérard C; Bordeleau L-J; Barralet J; Doillon CJ, The Stimulation of Angiogenesis and Collagen Deposition by Copper. *Biomaterials* 2010, 31 (5), 824–831. [PubMed: 19854506]
139. Wang L; Yang X; Cao W; Shi C; Zhou P; Li Q; Han F; Sun J; Xing X; Li B, Mussel-Inspired Deposition of Copper on Titanium for Bacterial Inhibition and Enhanced Osseointegration in a Periprosthetic Infection Model. *RSC Adv* 2017, 7 (81), 51593–51604.
140. Hong R; Kang TY; Michels CA; Gadura N Membrane lipid peroxidation in copper alloy-mediated contact killing of Escherichia coli. *Appl. Environ. Microbiol* 2012, 78 (6), 1776–1784. [PubMed: 22247141]
141. San K; Long J; Michels CA; Gadura N Antimicrobial Copper Alloy Surfaces are Effective Against Vegetative but not Sporulated Cells of Gram-positive Bacillus subtilis. *MicrobiologyOpen* 2015, 4 (5), 753–763. [PubMed: 26185055]
142. Zhang Y-M; Rock CO Membrane Lipid Homeostasis in Bacteria. *Nat. Rev. Microbiol* 2008, 6 (3), 222–233. [PubMed: 18264115]
143. Studer AM; Limbach LK; Van Duc L; Krumeich F; Athanassiou EK; Gerber LC; Moch H; Stark WJ Nanoparticle Cytotoxicity Depends on Intracellular Solubility: Comparison of Stabilized Copper Metal and Degradable Copper Oxide Nanoparticles. *Toxicol. Lett* 2010, 197 (3), 169–174. [PubMed: 20621582]
144. Stohs SJ; Bagchi D Oxidative Mechanisms in the Toxicity of Metal Ions. *Free Radic. Biol. Med* 1995, 18 (2), 321–336. [PubMed: 7744317]
145. Yamanaka M; Hara K; Kudo J Bactericidal Actions of a Silver ion Solution on Escherichia coli, Studied by Energy-filtering Transmission Electron Microscopy and Proteomic Analysis. *Appl. Environ. Microbiol* 2005, 71 (11), 7589–7593. [PubMed: 16269810]

146. Li M; Ma Z; Zhu Y; Xia H; Yao M; Chu X; Wang X; Yang K; Yang M; Zhang Y; Mao C Toward a Molecular Understanding of the Antibacterial Mechanism of Copper-Bearing Titanium Alloys against *Staphylococcus aureus*. *Adv. Healthcare Mater* 2016, 5 (5), 557–566.
147. McDevitt CA; Ogunniyi AD; Valkov E; Lawrence MC; Kobe B; McEwan AG; Paton JC A Molecular Mechanism for Bacterial Susceptibility to Zinc. *PLOS Pathog* 2011, 7 (11), e1002357. [PubMed: 22072971]
148. Campoccia D; Montanaro L; Arciola CR A Review of the Biomaterials Technologies for Infection-Resistant Surfaces. *Biomaterials* 2013, 34 (34), 8533–8554. [PubMed: 23953781]
149. Bondarenko O; Juganson K; Ivask A; Kasemets K; Mortimer M; Kahru A, Toxicity of Ag, CuO and ZnO Nanoparticles to Selected Environmentally Relevant test Organisms and Mammalian Cells In Vitro: a Critical Review. *Arch. Toxicol* 2013, 87 (7), 1181–1200. [PubMed: 23728526]
150. Gao A; Hang R; Huang X; Zhao L; Zhang X; Wang L; Tang B; Ma S; Chu PK, The Effects of Titania Nanotubes with Embedded Silver Oxide Nanoparticles on Bacteria and Osteoblasts. *Biomaterials* 2014, 35 (13), 4223–4235. [PubMed: 24529392]
151. C Chouirfa H; Bouloussa H; Migonney V; Falentin-Daudré C Review of Titanium Surface Modification Techniques and Coatings for Antibacterial Applications. *Acta Biomater* 2019, 83, 37–54. [PubMed: 30541702]
152. Lichter JA; Van Vliet KJ; Rubner MF, Design of Antibacterial Surfaces and Interfaces: Polyelectrolyte Multilayers as a Multifunctional Platform. *Macromolecules* 2009, 42 (22), 8573–8586.
153. Yeh M-L; Chen K-H; Chang N-J; Chen H-D; Lai K-A Prolonged Antibiotic Release by PLGA Encapsulation on Titanium Alloy. *J. Med. Biol. Eng* 2013, 33, 17–22.
154. Pichavant L; Amador G; Jacqueline C; Brouillaud B; Heroguez V; Durrieu MC pH-Controlled Delivery of Gentamicin Sulfate from Orthopedic Devices Preventing Nosocomial Infections. *J. Control. Release* 2012, 162 (2), 373–81. [PubMed: 22771533]
155. Lawson MC; Bowman CN; Anseth KS Vancomycin Derivative Photopolymerized to Titanium Kills *S. epidermidis*. *Clin. Orthop. Relat. Res* 2007, 461.
156. Zhang F; Shi ZL; Chua PH; Kang ET; Neoh KG Functionalization of Titanium Surfaces via Controlled Living Radical Polymerization: From Antibacterial Surface to Surface for Osteoblast Adhesion. *Ind. Eng. Chem. Res* 2007, 46 (26), 9077–9086.
157. Lee D-W; Yun Y-P; Park K; Kim SE Gentamicin and Bone Morphogenic Protein-2 (BMP-2)-delivering Heparinized-titanium Implant with Enhanced Antibacterial Activity and Osteointegration. *Bone* 2012, 50 (4), 974–982. [PubMed: 22289658]
158. Yuan Z; Huang S; Lan S; Xiong H; Tao B; Ding Y; Liu Y; Liu P; Cai K Surface Engineering of Titanium Implants with Enzyme-triggered Antibacterial Properties and Enhanced Osseointegration *in vivo*. *J. Mater. Chem. B* 2018, 6 (48), 8090–8104. [PubMed: 32254929]
159. Wang T; Liu X; Zhu Y; Cui ZD; Yang XJ; Pan H; Yeung KWK; Wu S Metal Ion Coordination Polymer-Capped pH-Triggered Drug Release System on Titania Nanotubes for Enhancing Self-antibacterial Capability of Ti Implants. *ACS Biomater. Sci. Eng* 2017, 3 (5), 816–825. [PubMed: 33440485]
160. Wang T; Wang C; Zhou S; Xu J; Jiang W; Tan L; Fu J Nanovalves-Based Bacteria-Triggered, Self-Defensive Antibacterial Coating: Using Combination Therapy, Dual Stimuli-Responsiveness, and Multiple Release Modes for Treatment of Implant-Associated Infections. *Chem. Mater* 2017, 29 (19), 8325–8337.
161. Wu T-Y; Zhou Z-B; He Z-W; Ren W-P; Yu X-W; Huang Y Reinforcement of a New Calcium Phosphate Cement with RGD-chitosan-fiber. *J. Biomed. Mater. Res. A* 2014, 102 (1), 68–75. [PubMed: 23606446]
162. Wu T; Zhang Q; Ren W; Yi X; Zhou Z; Peng X; Yu X; Lang M Controlled Release of Gentamicin from Gelatin/Genipin Reinforced Beta-tricalcium Phosphate Scaffold for the Treatment of Osteomyelitis. *J. Mater. Chem. B* 2013, 1 (26), 3304–3313. [PubMed: 32261039]
163. Stigter M; Bezemer J; de Groot K; Layrolle P Incorporation of Different Antibiotics into Carbonated Hydroxyapatite Coatings on Titanium Implants, Release and Antibiotic Efficacy. *J. Control. Release* 2004, 99 (1), 127–137. [PubMed: 15342186]

164. Zhang L; Ning C; Zhou T; Liu X; Yeung KW; Zhang T; Xu Z; Wang X; Wu S; Chu PK Polymeric Nanoarchitectures on Ti-based Implants for Antibacterial Applications. *ACS Appl. Mater. Interfaces* 2014, 6 (20), 17323–17345. [PubMed: 25233376]
165. Zilberman M; Elsner JJ Antibiotic-eluting Medical Devices for Various Applications. *J. Control. Release* 2008, 130 (3), 202–215. [PubMed: 18687500]
166. Zhou Z; Seta J; Markel DC; Song W; Yurgelevic SM; Yu XW; Ren W Release of Vancomycin and Tobramycin from Polymethylmethacrylate Cements Impregnated with Calcium Polyphosphate Hydrogel. *J. Biomed. Mater. Res. B, Appl. Biomater* 2018, 106 (8), 2827–2840. [PubMed: 29282858]
167. Poole K Mechanisms of Bacterial Biocide and Antibiotic Resistance. *J. Appl. Microbiol* 2002, 92 Suppl, 55s–64s. [PubMed: 12000613]
168. Alarcón C. d. l. H.; Pennadam S; Alexander C Stimuli Responsive Polymers for Biomedical Applications. *Chem. Soc. Rev* 2005, 34 (3), 276–285. [PubMed: 15726163]
169. Tang F; Li L; Chen D Mesoporous Silica Nanoparticles: Synthesis, Biocompatibility and Drug Delivery. *Adv. Mater* 2012, 24 (12), 1504–1534. [PubMed: 22378538]
170. Kumar C; Chaudhari A Efficient Renaturation of Immobilized Met-hemoglobin at the Galleries of  $\alpha$ -zirconium Phosphonate. *Chem. Mater* 2001, 13 (2), 238–240.
171. Kumar CV; Chaudhari A Proteins Immobilized at the Galleries of Layered  $\alpha$ -zirconium Phosphate: Structure and Activity Studies. *J. Am. Chem. Soc* 2000, 122 (5), 830–837.
172. Li Z; Yuan D; Jin G; Tan BH; He C Facile Layer-by-Layer Self-Assembly toward Enantiomeric Poly(lactide) Stereocomplex Coated Magnetite Nanocarrier for Highly Tunable Drug Deliveries. *ACS Appl. Mater. Interfaces* 2016, 8 (3), 1842–1853. [PubMed: 26717323]
173. Zhou J; Horev B; Hwang G; Klein MI; Koo H; Benoit DS Characterization and Optimization of pH-responsive Polymer Nanoparticles for Drug Delivery to Oral Biofilms. *J. Mater. Chem. B* 2016, 4 (18), 3075–3085. [PubMed: 27429754]
174. Xiang Y; Liu X; Mao C; Liu X; Cui Z; Yang X; Yeung KW; Zheng Y; Wu S Infection-Prevention on Ti Implants by Controlled Drug Release from Folic acid/ZnO Quantum dots Sealed Titania Nanotubes. *Mater. Sci. Eng. C* 2018, 85, 214–224.
175. Zhao J; Xu J; Jian X; Xu J; Gao Z; Song Y-Y NIR Light-Driven Photocatalysis on Amphiphilic TiO<sub>2</sub> Nanotubes for Controllable Drug Release. *ACS Appl. Mater. & Interfaces* 2020, 12 (20), 23606–23616. [PubMed: 32356964]
176. Tao B; Deng Y; Song L; Ma W; Qian Y; Lin C; Yuan Z; Lu L; Chen M; Yang X; Cai K BMP2-loaded Titania Nanotubes Coating with pH-responsive Multilayers for Bacterial Infections Inhibition and Osteogenic Activity Improvement. *Colloids Surf. B Biointerfaces* 2019, 177, 242–252. [PubMed: 30763789]
177. Dong Y; Ye H; Liu Y; Xu L; Wu Z; Hu X; Ma J; Pathak JL; Liu J; Wu G pH Dependent Silver Nanoparticles Releasing Titanium Implant: A Novel Therapeutic Approach to Control Peri-implant Infection. *Colloids Surf. B Biointerfaces* 2017, 158, 127–136. [PubMed: 28688362]
178. Zhang T; Xie C; Liu Y; Zhang F; Xiao X pH-responsive Drug Release System of Cu<sup>2+</sup>-Modified Ammoniated TiO<sub>2</sub> Nanotube Arrays. *Mater. Lett* 2018, 215, 95–98.
179. Tao B; Zhao W; Lin C; Yuan Z; He Y; Lu L; Chen M; Ding Y; Yang Y; Xia Z; Cai K Surface Modification of Titanium Implants by ZIF-8@Levo/LBL Coating for Inhibition of Bacterial-associated Infection and Enhancement of In Vivo Osseointegration. *Chem. Eng. J* 2020, 390, 124621.
180. Cloutier M; Mantovani D; Rosei F Antibacterial Coatings: Challenges, Perspectives, and Opportunities. *Trends Biotechnol* 2015, 33 (11), 637–652. [PubMed: 26463723]
181. Noble ML; Mourad PD; Ratner BD Digital Drug Delivery: on–off Ultrasound Controlled Antibiotic Release from Coated Matrices with Negligible Background Leaching. *Biomater. Sci* 2014, 2 (6), 893–902.
182. Johnson CT; Wroe JA; Agarwal R; Martin KE; Guldborg RE; Donlan RM; Westblade LF; García AJ Hydrogel Delivery of Lysostaphin Eliminates Orthopedic Implant Infection by *Staphylococcus aureus* and Supports Fracture Healing. *PNAS* 2018, 115 (22), E4960. [PubMed: 29760099]

183. Yu Y; Ran Q; Shen X; Zheng H; Cai K Enzyme Responsive Titanium Substrates with Antibacterial Property and Osteo/Angio-genic Differentiation Potentials. *Colloids Surf. B Biointerfaces* 2020, 185, 110592. [PubMed: 31639570]
184. Kazemzadeh-Narbat M; Lai BF; Ding C; Kizhakkedathu JN; Hancock RE; Wang R, Multilayered Coating on Titanium for Controlled Release of Antimicrobial Peptides for the Prevention of Implant-associated Infections. *Biomaterials* 2013, 34 (24), 5969–77. [PubMed: 23680363]
185. Shen X; Zhang F; Li K; Qin C; Ma P; Dai L; Cai K, Cecropin B Loaded TiO<sub>2</sub> Nanotubes Coated with Hyaluronidase Sensitive Multilayers for Reducing Bacterial Adhesion. *Mater. Des* 2016, 92, 1007–1017.
186. Ramesh S; Govender T; Kruger HG; de la Torre BG; Albericio F, Short AntiMicrobial Peptides (SAMPs) as a Class of Extraordinary Promising Therapeutic Agents. *J. Pept. Sci* 2016, 22 (7), 438–451. [PubMed: 27352996]
187. Chen CH; Lu TK, Development and Challenges of Antimicrobial Peptides for Therapeutic Applications. *Antibiotics (Basel)* 2020, 9 (1), 24.
188. Carmona G; Rodriguez A; Juarez D; Corzo G; Villegas E, Improved Protease Stability of the Antimicrobial Peptide Pin2 Substituted with d-Amino Acids. *Protein J* 2013, 32 (6), 456–466. [PubMed: 23925670]
189. Ron-Doitch S; Sawodny B; Kühbacher A; David MMN; Samanta A; Phopase J; Burger-Kentischer A; Griffith M; Golomb G; Rupp S, Reduced Cytotoxicity and Enhanced Bioactivity of Cationic Antimicrobial Peptides Liposomes in Cell Cultures and 3D Epidermis Model Against HSV. *J. Control. Release* 2016, 229, 163–171. [PubMed: 27012977]
190. Touti F; Lautrette G; Johnson KD; Delaney JC; Wollacott A; Tissire H; Viswanathan K; Shriver Z; Mong SK; Mijalis AJ; Plante OJ; Pentelute BL, Antibody-Bactericidal Macrocylic Peptide Conjugates To Target Gram-Negative Bacteria. *ChemBioChem* 2018, 19 (19), 2039–2044. [PubMed: 29984452]
191. Wang C; Wang Y; Zhang L; Miron RJ; Liang J; Shi M; Mo W; Zheng S; Zhao Y; Zhang Y Pretreated Macrophage-Membrane-Coated Gold Nanocages for Precise Drug Delivery for Treatment of Bacterial Infections. *Adv. Mater* 2018, 30 (46), 1804023.
192. Hu D; Li H; Wang B; Ye Z; Lei W; Jia F; Jin Q; Ren K-F; Ji J Surface-Adaptive Gold Nanoparticles with Effective Adherence and Enhanced Photothermal Ablation of Methicillin-Resistant *Staphylococcus aureus* Biofilm. *ACS Nano* 2017, 11 (9), 9330–9339. [PubMed: 28806528]
193. Yin W; Yu J; Lv F; Yan L; Zheng LR; Gu Z; Zhao Y Functionalized Nano-MoS<sub>2</sub> with Peroxidase Catalytic and Near-Infrared Photothermal Activities for Safe and Synergetic Wound Antibacterial Applications. *ACS Nano* 2016, 10 (12), 11000–11011. [PubMed: 28024334]
194. Yuan Z; Tao B; He Y; Mu C; Liu G; Zhang J; Liao Q; Liu P; Cai K Remote Eradication of Biofilm on Titanium Implant via Near-Infrared Light Triggered Photothermal/Photodynamic Therapy Strategy. *Biomaterials* 2019, 223, 119479. [PubMed: 31520885]
195. He C; Duan X; Guo N; Chan C; Poon C; Weichselbaum RR; Lin W Core-shell Nanoscale Coordination Polymers Combine Chemotherapy and Photodynamic Therapy to Potentiate Checkpoint Blockade Cancer Immunotherapy. *Nat. Commun* 2016, 7 (1), 12499. [PubMed: 27530650]
196. Mao C; Xiang Y; Liu X; Cui Z; Yang X; Li Z; Zhu S; Zheng Y; Yeung KWK; Wu S Repeatable Photodynamic Therapy with Triggered Signaling Pathways of Fibroblast Cell Proliferation and Differentiation To Promote Bacteria-Accompanied Wound Healing. *ACS Nano* 2018, 12 (2), 1747–1759. [PubMed: 29376340]
197. Li X; Lee D; Huang J-D; Yoon J Phthalocyanine-Assembled Nanodots as Photosensitizers for Highly Efficient Type I Photoreactions in Photodynamic Therapy. *Angew. Chem. Int. Ed* 2018, 57 (31), 9885–9890.
198. Feng Z; Liu X; Tan L; Cui Z; Yang X; Li Z; Zheng Y; Yeung KWK; Wu S Electrophoretic Deposited Stable Chitosan@MoS<sub>2</sub> Coating with Rapid In Situ Bacteria-Killing Ability under Dual-Light Irradiation. *Small* 2018, 14 (21), 1704347.

199. Berman AT; Reid JS; Yanicko DR Jr.; Sih GC; Zimmerman MR, Thermally Induced Bone Necrosis in Rabbits. Relation to Implant Failure in Humans. *Clin. Orthop. Relat. Res* 1984, (186), 284–92. [PubMed: 6723155]
200. Li Y; Liu X; Li B; Zheng Y; Han Y; Chen D.-f.; Yeung KWK; Cui Z; Liang Y; Li Z; Zhu S; Wang X; Wu S Near-Infrared Light Triggered Phototherapy and Immunotherapy for Elimination of Methicillin-Resistant *Staphylococcus aureus* Biofilm Infection on Bone Implant. *ACS Nano* 2020, 14 (7), 8157–8170. [PubMed: 32585104]
201. Raphael J; Holodniy M; Goodman SB; Heilshorn SC, Multifunctional Coatings to Simultaneously Promote Osseointegration and Prevent Infection of Orthopaedic Implants. *Biomaterials* 2016, 84, 301–314. [PubMed: 26851394]
202. Mas-Moruno C; Su B; Dalby MJ, Multifunctional Coatings and Nanotopographies: Toward Cell Instructive and Antibacterial Implants. *Adv. Healthc. Mater* 2019, 8 (1), e1801103. [PubMed: 30468010]
203. An YH; Friedman RJ, Animal Models of Orthopedic Implant Infection. *J. Invest. Surg* 1998, 11 (2), 139–46. [PubMed: 9700622]
204. An YH; Kang QK; Arciola CR, Animal Models of Osteomyelitis. *Int. J. Artif. Organs* 2006, 29 (4), 407–20. [PubMed: 16705610]
205. Gatin L; Saleh-Mghir A; Massin P; Cremieux AC, Critical analysis of experimental models of periprosthetic joint infection. *Orthop Traumatol Surg Res* 2015, 101 (7), 851–5. [PubMed: 26454411]
206. Bottagisio M; Coman C; Lovati AB, Animal Models of Orthopaedic Infections. A Review of Rabbit Models used to Induce Long Bone Bacterial Infections. *J. Med. Microbiol* 2019, 68, 506–537. [PubMed: 30875284]
207. Jie K; Deng P; Cao H; Feng W; Chen J; Zeng Y, Prosthesis Design of Animal Models of Periprosthetic Joint infection Following Total Knee Arthroplasty: A Systematic Review. *PLoS One* 2019, 14 (10), e0223402. [PubMed: 31581252]

**Figure 1.**

(A) Anti-fouling or QS-interfering surface modification strategies designed to inhibit bacterial adhesion, colonization and biofilm formation. These strategies involve coating surfaces with hydrophilic polymers, engineering superhydrophobic nanostructured surface topography to emulate the lotus leaf effect or applying coatings that release agents interfering with QS. (B) Bactericidal surface modification strategies designed to kill bacteria in direct contact with the surface and/or those in its vicinity. These strategies involve engineering nanostructured surface topography capable of physically rupturing bacteria, covalently tethering bactericidal agents to the surface with stable linkages or linkages labile to bacterial enzyme cleavage or pH perturbations, physically encapsulating bactericidal agents in surface coatings for passive releases, or applying photothermal/photodynamic responsive coatings (e.g. in response to near-infrared, or NIR, irradiation) designed to destruct established biofilms.

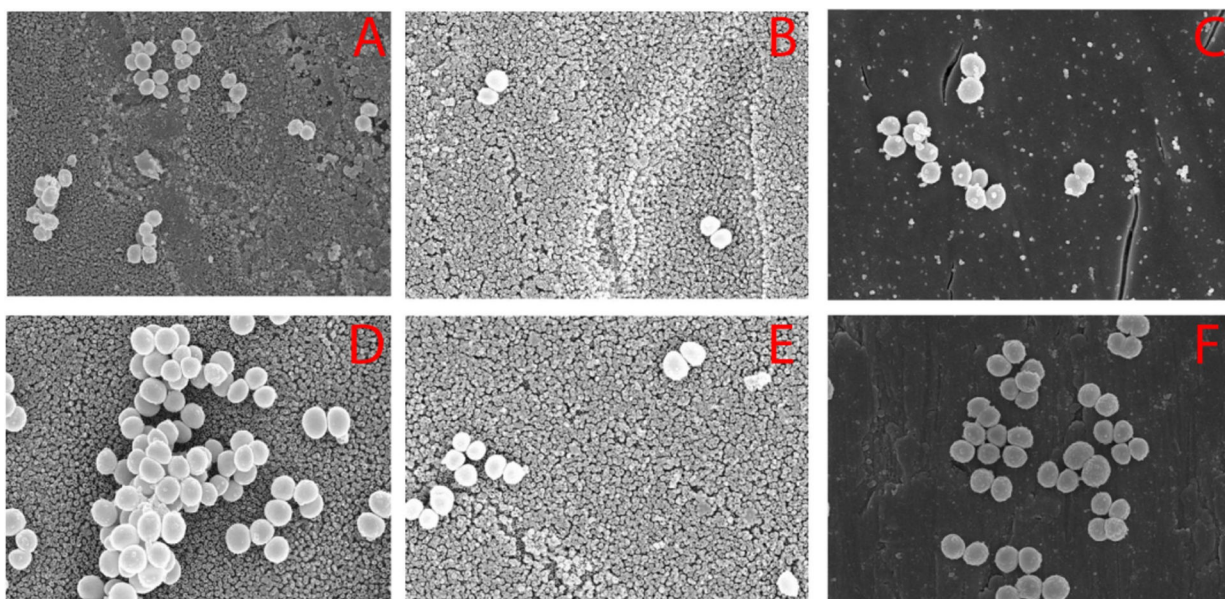


**Figure 2.** SEM images of bacteria colonies after 2h on (A) NT, (B) NTS, and (C) TiS, and after 4h (D) NT, (E) NTS, and (F) TiS ( $\times 10K$ ). Reproduced with the permission from ref 59. Copyright 2011 Hindawi.

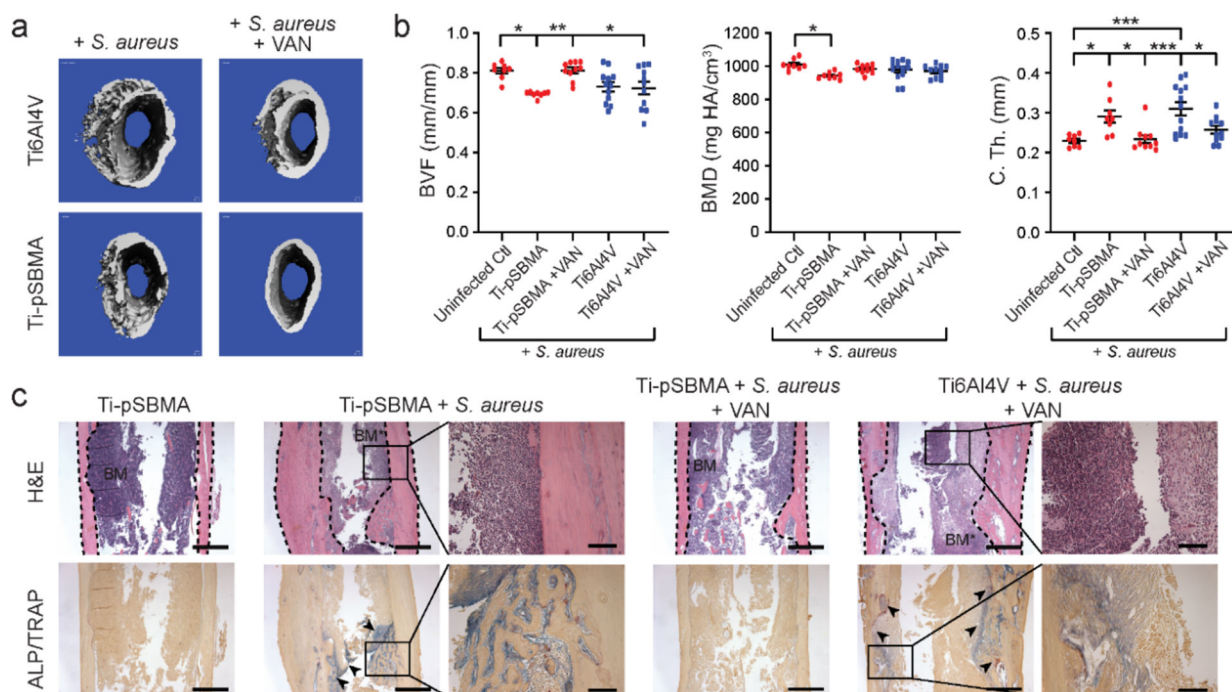


**Figure 3.** pSBMA grafted from the surface of Ti6Al4V IM pins combined with a single vancomycin injection (Ti-pSBMA+VAN) more effectively suppressed *S. aureus* periprosthetic infection in mouse femoral canals than pSBMA coating alone (Ti-pSBMA) or the single systemic vancomycin injection alone (Ti6Al4V+VAN). (a)  $\mu$ -CT axial view of the femur at day 21 (pins contoured out). (b)  $\mu$ -CT quantitation of bone volume fraction (BVF), bone mineral density (BMD) and cortical thickness (C. Th) at day 21. \* $P$ <0.05, \*\* $P$ <0.01, \*\*\* $P$ <0.001. All femurs were inoculated with 40-CFU Xen 29 prior to pin insertion. Reproduced with the permission from ref 93. Copyright 2020 American Chemical Society.



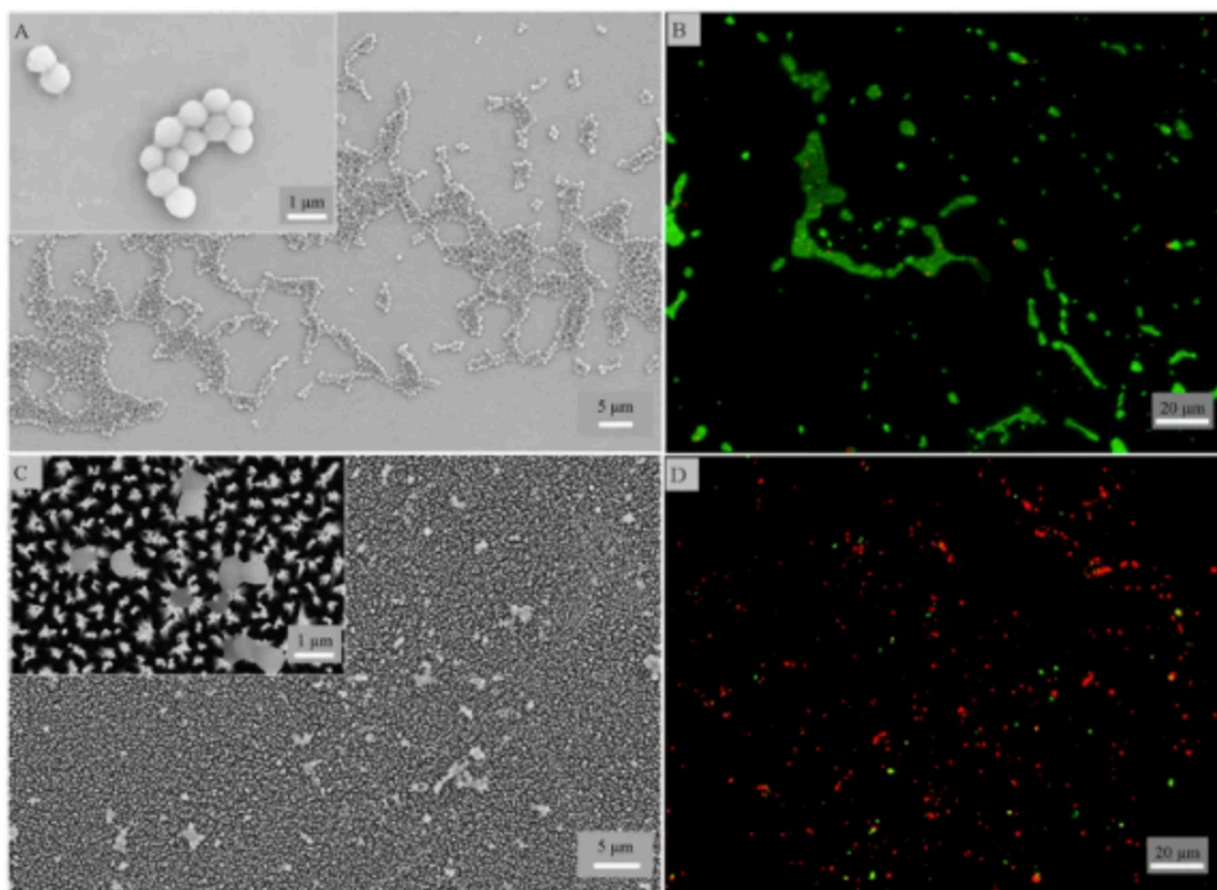


**Figure 4.** (A-D) SEM and fluorescence images of *S. aureus* attached for 24 h on the control (top) and black titanium (bottom) surfaces. Insets in panels A and C: enlarged views of live and dead bacteria on the respective surfaces. Reproduced with the permission from ref 105. Copyright 2017 Springer Nature.

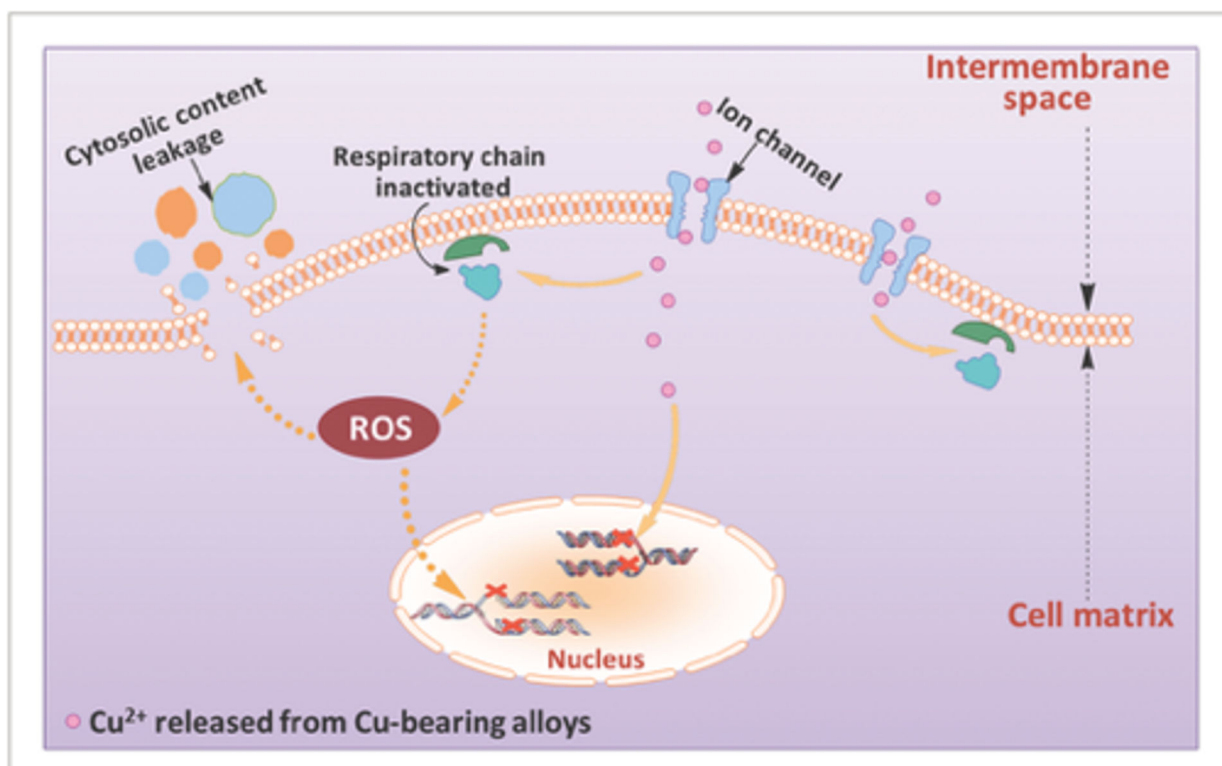


**Figure 5.** Schematic illustration of possible antibacterial mechanisms on the surface of Ti6Al4V5Cu implants. Ti6Al4V5Cu releases Cu ions. The released Cu ions could accumulate in the cell membrane affecting membrane permeability, disrupt the activity of respiratory chain, enter bacterial cells to generate ROS, and disrupt the gene replication of *S. aureus*. Reproduced with the permission from ref 146. Copyright 2015 Wiley Publication.

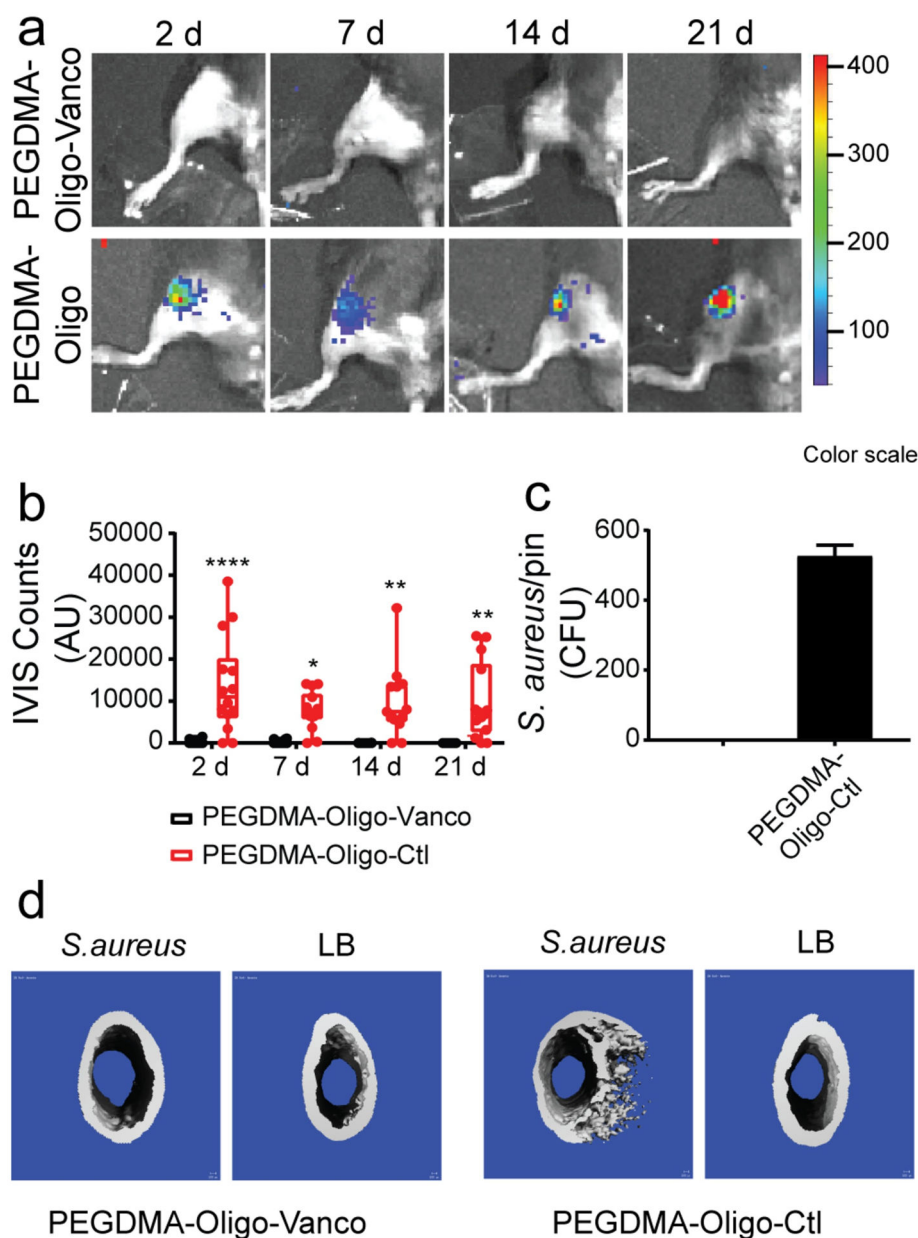


**Figure 6.** (a) IVIS images of mouse femurs injected with 40 CFU Xen-29 *S. aureus* and inserted with IM pins with PEGDMA-Oligo-Vanco or PEGDMA-Oligo coatings at 2, 7, 14, and 21 days. (b) Quantification of longitudinal bioluminescence signals of mouse femurs injected with 40 CFU Xen-29 *S. aureus* and inserted with the different hydrogel-coated pins at 2, 7, 14, and 21 days ( $n = 14$ ). (c) *S. aureus* recovery from explanted pins at 21 days ( $n = 11$ ). (d) 3D  $\mu$ CT axial images of the distal femoral region 21 days after the insertion of Ti6Al4V IM pins (pins excluded during contouring) with different hydrogel coatings, with or without the inoculation of 40-CFU Xen-29 *S. aureus*. Error bars represent standard deviations. \*  $p$  0.05, \*\*  $p$  0.01, \*\*\*  $p$  0.001, \*\*\*\*  $p$  0.0001 (two-way ANOVA for part b; Student's  $t$ -

test for part c). Reproduced with the permission from ref 21. Copyright 2019 American Chemical Society.

Author Manuscript

Author Manuscript

Author Manuscript

Author Manuscript